

Abstract

Here we explore the potential of time-series magnesium ($\delta^{26}\text{Mg}$) isotope data as continental climate proxies in speleothem calcite archives. For this purpose, a total of six Pleistocene and Holocene stalagmites from caves in Germany, Morocco and Peru and two flowstones from a cave in Austria were investigated. These caves represent the semi-arid to arid (Morocco), the warm-temperate (Germany), the equatorial-humid (Peru) and the cold-humid (Austria) climate zones. Changes in the calcite magnesium isotope signature with time are placed against carbon and oxygen isotope records from these speleothems. Similar to other proxies, the non-trivial interaction of a number of environmental, equilibrium and non-equilibrium processes governs the $\delta^{26}\text{Mg}$ fractionation in continental settings. These include the different sources of magnesium isotopes such as rain water or snow as well as soil and hostrock, soil zone biogenic activity, shifts in silicate versus carbonate weathering ratios and residence time of water in the soil and karst zone. Pleistocene stalagmites from Morocco show the lowest mean $\delta^{26}\text{Mg}$ values (GDA: $-4.26 \pm 0.07\text{‰}$ and HK3: $-4.17 \pm 0.15\text{‰}$) and the data are well explained in terms of changes in aridity over time. The Pleistocene to Holocene stalagmites from Peru show the highest mean value (NC-A and NC-B $\delta^{26}\text{Mg}$: $-3.96 \pm 0.04\text{‰}$) but only minor variations in Mg-isotope composition, which is in concert with the rather stable equatorial climate at this site. Holocene stalagmites from Germany (AH-1 mean $\delta^{26}\text{Mg}$: $-4.01 \pm 0.07\text{‰}$; BU 4 mean $\delta^{26}\text{Mg}$: $-4.20 \pm 0.10\text{‰}$) record changes in outside air temperature as driving factor rather than rainfall amount. The alpine Pleistocene flowstones from Austria (SPA 52: $-3.00 \pm 0.73\text{‰}$; SPA 59: $-3.70 \pm 0.43\text{‰}$) are affected by glacial versus interglacial climate change with outside air temperature affecting soil zone activity and weathering balance. Several data points in the Austrian and two data points in the German speleothems are shifted to higher values due to sampling in detrital layers (Mg-bearing clay minerals) of the speleothems. The data and their interpretation shown here highlight the potential but also the limitations of the magnesium isotope proxy applied in continental climate research. An

The magnesium isotope record of cave carbonate archives

S. Riechelmann et al.

Title Page

Abstract

Introduction

Conclusions

References

Tables

Figures

⏪

⏩

◀

▶

Back

Close

Full Screen / Esc

Printer-friendly Version

Interactive Discussion



obvious potential lies in its sensitivity for even subtle changes in soil-zone parameters, a hitherto rather poorly understood but extremely important component in cave archive research. Limitations are most obvious in the low resolution and high sample amount needed for analysis. Future research should focus on experimental and conceptual aspects including quantitative and well calibrated leaching and precipitation experiments.

1 Introduction

Carbon and oxygen isotope ratios as well as trace elemental abundances are widely used proxy data from speleothem archives (e.g. Genty and Massault, 1999; Spötl et al., 2002; Lachniet et al., 2004; Cruz et al., 2007; Fairchild and McMillian, 2007; Scholz et al., 2009; Rudzka et al., 2011). The factors that control speleothem geochemistry include ambient environmental parameters (Baker and Genty, 1998; Spötl et al., 2005; Baldini et al., 2008), carbonate mineralogy (Frisia et al., 2000, 2002; Frisia and Borsato, 2010), as well as equilibrium and disequilibrium conditions in the aquifer (Tooth and Fairchild, 2003; Miorandi et al., 2010; Sherwin and Baldini, 2011) and during speleothem precipitation in the cave (White, 2004; Tremaine et al., 2011; Riechelmann et al., 2012a).

Despite significant advances in field studies (Spötl et al., 2005; Asrat et al., 2008; Verheyden et al., 2008; Riechelmann et al., 2011), including experimental (Huang and Fairchild, 2001; Collister and Matthey, 2008; Polag et al., 2010) and numerical (Mühlinghaus et al., 2007; DePaolo, 2011; Dreybrodt and Scholz, 2011) work, several parameters that affect proxy data remain difficult to constrain. In this respect, validation of proxy data from individual coeval stalagmites within a given cave (Dorale et al., 1998; Vollweiler et al., 2006) and between different caves (Williams et al., 2004; Mangini et al., 2005; Fohlmeister et al., 2012) is a key issue.

More recently, it has been proposed that multi-proxy studies including novel approaches such as fluid inclusions, noble gases, clumped isotopes and non-traditional isotope systems (Kluge et al., 2008; Scheidegger et al., 2008; Immenhauser et al.,

CPD

8, 1835–1883, 2012

The magnesium isotope record of cave carbonate archives

S. Riechelmann et al.

Title Page

Abstract

Introduction

Conclusions

References

Tables

Figures

⏪

⏩

◀

▶

Back

Close

Full Screen / Esc

Printer-friendly Version

Interactive Discussion



The magnesium isotope record of cave carbonate archives

S. Riechelmann et al.

Title Page

Abstract

Introduction

Conclusions

References

Tables

Figures

◀

▶

◀

▶

Back

Close

Full Screen / Esc

Printer-friendly Version

Interactive Discussion



2010; Daëron et al., 2011; Reynard et al., 2011) may provide valuable information and complement more traditional proxy data. Amongst these more recently established proxies are Mg isotope ($\delta^{26}\text{Mg}$) data. Previous work dealing with Mg isotope fractionation in Earth surface environments includes investigations from carbonate archives and field and laboratory precipitation experiments. Data available in the literature include $\delta^{26}\text{Mg}$ ratios from rain, snow, riverine, soil and drip water as well as hostrock and cave carbonates and soil and cave silicate data (Galy et al., 2002; Young and Galy, 2004; de Villiers et al., 2005; Tipper et al., 2006b, 2008, 2010; Buhl et al., 2007; Brenot et al., 2008; Immenhauser et al., 2010; Pokrovsky et al., 2011; Riechelmann et al., 2012b). Nevertheless, with the exception of the preliminary work shown in Buhl et al. (2007), a critical application of the above-cited work to speleothem time series data is lacking.

Here we report on the potential and limitations of Mg isotope time series proxy data interpretation from eight speleothems collected in six caves on three different continents. The goals of this study are to (1) review parameters known to affect $\delta^{26}\text{Mg}$ fractionation between land surface and cave carbonate deposition, to (2) apply these findings to all available $\delta^{26}\text{Mg}$ time-series data sets from Pleistocene/Holocene speleothems and flowstones.

2 Case settings

This study makes use of $\delta^{26}\text{Mg}$ isotope data from six stalagmites and two flowstones. These include two stalagmites from Germany (Atta Cave and Bunker Cave), two stalagmites from Morocco (Grotte d'Aoufous and Grotte Prison de Chien), two stalagmites from Peru (Cueva del Tigre Perdido) and two flowstones from Austria (Spannagel Cave). The reader is referred to Fig. 1 and Table 1 for detailed information regarding cave parameters and speleothems investigated.

3 Magnesium isotope analysis

Powder subsamples from longitudinally cut stalagmites and flowstones were dissolved in 6 M HCl. The solution was dried and re-dissolved with 250 μ l of a 1 : 1 mixture of HNO₃: H₂O₂ (65% : 31%). Subsequently, the solution was evaporated and again re-dissolved in 1.25 M HCl. The Mg-bearing fraction was extracted by using ion-exchange columns (BioRad ion exchange resin AG50 W-X12, 200 to 400 mesh), evaporated to dryness and a 500 ppb Mg-solution (in 3.5 % HNO₃) was prepared. The samples were analyzed with a Thermo Fisher Scientific Neptune MC-ICP-MS using DSM3 standard solution. The external precision was determined by measuring the mono-elemental solution Cambridge 1 repeatedly ($n = 89$, $\delta^{25}\text{Mg}$: $-1.34 \pm 0.01\text{‰}$ and $\delta^{26}\text{Mg}$: $-2.58 \pm 0.03\text{‰}$). For details of the analytical procedure refer to Immenhauser et al. (2010).

The stalagmite AH-1 (Atta Cave) provided material that was tested for the impact of fluid inclusions in the calcite fabric on the bulk $\delta^{26}\text{Mg}$. The sample was taken because it contains numerous fluid inclusions. Calcite samples from this stalagmite were extracted and half of each sample grounded in acetone to remove the fluid inclusions and subsequently analysed for their magnesium isotope signature. Aliquots of non-treated samples were analysed too and results compared.

4 Speleothem geochemistry: results

Carbon and oxygen isotope time series data as well as U-Th age data shown in Figs. 3 and 5–10 are published in Niggemann et al. (2003), Holzkämper et al. (2005), Buhl et al. (2007), Spötl et al. (2007), van Breukelen et al. (2008), van Breukelen (2009), Wassenburg et al. (2012) and Fohlmeister et al. (2012). Time series stalagmite and flowstone Mg isotope data are shown in Tables 2 and 3 and Fig. 2. Below, the main geochemical characteristics are summarized for each speleothem analyzed.

Moroccan stalagmites GDA and HK3 and stalagmite BU 4 from Germany yielded the most depleted mean values, whilst flowstones SPA 52 and SPA 59 from Austria

CPD

8, 1835–1883, 2012

The magnesium isotope record of cave carbonate archives

S. Riechelmann et al.

Title Page

Abstract

Introduction

Conclusions

References

Tables

Figures

◀

▶

◀

▶

Back

Close

Full Screen / Esc

Printer-friendly Version

Interactive Discussion

are least depleted in terms of their mean $\delta^{26}\text{Mg}$ signatures. Stalagmite AH-1 from Germany and the Peruvian stalagmites NC-A and NC-B yielded intermediate mean $\delta^{26}\text{Mg}$ values (Fig. 2). The flowstones SPA 52 and SPA 59 show the highest variations in their Mg-isotope composition. In contrast, stalagmite $\delta^{26}\text{Mg}$ is less variable. Stalagmite HK3 (Morocco) and stalagmite BU 4 (Germany) show the highest amplitudes in $\delta^{26}\text{Mg}$, whilst stalagmites NC-A and NC-B (Peru) reveal the lowest degree of variability and therefore the smallest $\Delta^{26}\text{Mg}$. Stalagmites AH-1 (Germany) and GDA (Morocco) show intermediate amplitudes (Fig. 2).

4.1 Stalagmite AH-1, Atta Cave, Germany

Holocene to recent (1997 AD) stalagmite AH-1 $\delta^{26}\text{Mg}$ values range from $-4.18 \pm 0.05\text{‰}$ to $-3.86 \pm 0.03\text{‰}$ with a mean of $-4.01 \pm 0.07\text{‰}$ (Figs. 2 and 3a, Tables 2 and 3). Stalagmite AH-1 yielded overall more depleted values between 9.0 and 6.0 ka BP and less depleted values between 6.0 and 0.7 ka BP. Between 6.0 and 4.2 ka BP, a trend to lower $\delta^{26}\text{Mg}$ values is observed and between 9.0 to 6.0 ka BP and 4.2 to 0.7 ka BP, a weak trend to ^{26}Mg -enriched values and a higher overall variability is found. The lowest $\delta^{26}\text{Mg}$ value is found at 8.7 ka BP. An enriched $\delta^{26}\text{Mg}$ value at 7.9 ka BP coincides with a detritus layer. Between 4.2 to 3.5 ka BP, a trend to higher values is found. At 3.2 ka BP, the $\delta^{26}\text{Mg}$ value becomes slightly depleted whilst subsequently the value is again more enriched at 2.5 ka BP. Between 2.5 and 1.6 ka BP $\delta^{26}\text{Mg}$ values decrease again and then increase between 1.6 and 1.5 ka BP. At 1.5 ka BP the least depleted $\delta^{26}\text{Mg}$ ratio is present. At 1.2 ka BP, $\delta^{26}\text{Mg}$ show again a more depleted value whilst the most recent data point, dated at 0.7 ka BP is less depleted.

The results from the fluid inclusion test runs are presented in Table 4 and Fig. 4. The $\Delta^{26}\text{Mg}$ between bulk (with intact fluid inclusions) and grounded samples (without fluid inclusions) is not exceeding the second decimal. Nevertheless, grounded samples are systematically lower by 0.01 to 0.08 ‰ in their Mg-isotope composition relative to their aliquots containing fluid inclusions (Fig. 4). Error bars of all these samples,

The magnesium isotope record of cave carbonate archives

S. Riechelmann et al.

Title Page

Abstract

Introduction

Conclusions

References

Tables

Figures

⏪

⏩

◀

▶

Back

Close

Full Screen / Esc

Printer-friendly Version

Interactive Discussion



however, exceed the $\Delta^{26}\text{Mg}$ and therefore, the potential impact of fluid inclusions on calcite $\delta^{26}\text{Mg}$ is not considered of significance here.

4.2 Stalagmite BU 4, Bunker Cave, Germany

Holocene to recent (2007 AD) stalagmite BU 4 $\delta^{26}\text{Mg}$ values range from $-4.34 \pm 0.07\%$ to $-3.91 \pm 0.05\%$ with a mean value of $-4.20 \pm 0.10\%$ (Figs. 2 and 5a, Tables 2 and 3). Between 8.2 and 7.8 ka BP, a trend towards lower values is found that is inverted at around 7.6 ka BP. More depleted $\delta^{26}\text{Mg}$ values are again observed between 7.0 and 6.0 ka BP. The least depleted $\delta^{26}\text{Mg}$ value coincide with a hiatus marked by coralloid layer and detrital material dated 5.5 ka BP. Subsequent speleothem calcite precipitated between 3.9 to 1.8 ka BP with decreasing $\delta^{26}\text{Mg}$ values. Between 1.8 and 1.1 ka BP, $\delta^{26}\text{Mg}$ values are invariant with one higher value at 1.1 ka BP. The lowest measured value was dated 0.4 ka BP. Subsequently, $\delta^{26}\text{Mg}$ ratios are slightly less depleted.

4.3 Stalagmites NC-A and NC-B, Cueva del Tigre Perdido, Peru

Upper Pleistocene to recent stalagmites NC-A and NC-B $\delta^{26}\text{Mg}$ values range from $-4.03 \pm 0.04\%$ to $-3.88 \pm 0.03\%$ with a mean of $-3.96 \pm 0.04\%$ (Figs. 2 and 6a, Tables 2 and 3). Magnesium isotope values in speleothem NC-B (13.1 to 3.6 ka) are invariant with fluctuations mostly within the analytical error. Speleothem NC-A $\delta^{26}\text{Mg}$ value is slightly enriched at 2.8 ka BP and at 1.9 ka BP the value is ^{26}Mg -depleted. The last point at 0.06 ka BP is again ^{26}Mg -enriched. These shifts, however, barely exceed the error bars of NC-B.

4.4 Stalagmite GDA, Grotte d'Aoufous, Morocco

Pleistocene ($2.134 \pm 0.115\text{Ma}$, Table 1) stalagmite GDA $\delta^{26}\text{Mg}$ values range from $-4.39 \pm 0.02\%$ to $-4.17 \pm 0.05\%$ with a mean value of $-4.26 \pm 0.07\%$ (Figs. 2 and 7a, Tables 2 and 3). Age dating was performed by the U-Pb method (measured at

CPD

8, 1835–1883, 2012

The magnesium isotope record of cave carbonate archives

S. Riechelmann et al.

Title Page

Abstract

Introduction

Conclusions

References

Tables

Figures

⏪

⏩

◀

▶

Back

Close

Full Screen / Esc

Printer-friendly Version

Interactive Discussion



the University of Berne, Switzerland), therefore error bars are large. From the base of the stalagmite GDA $\delta^{26}\text{Mg}$ values show more depleted values in the lower third of the stalagmite; i.e. between 13.6 and 9.7 cm distance from the top (dft) of the stalagmite. At 8.9 cm dft, i.e. the middle part, a more ^{26}Mg -enriched value is recorded reaching plateau values between 8.9 and 7.7 cm dft. The magnesium isotope value is again more enriched at 6.3 dft and a second plateau phase is reached between 6.3 and 3.1 cm dft, whilst $\delta^{26}\text{Mg}$ is again depleted at 2.3 cm dft.

4.5 Stalagmite HK3, Grotte Prison de Chien, Morocco

The Pleistocene to Holocene stalagmite HK3 consists of several primary aragonitic and calcitic layers reflecting alternately more arid (aragonite) and less arid (calcite) climate conditions. Data from samples across two transitions from aragonite to calcite and from calcite to aragonite are used and were described in detail in Wassenburg et al. (2012). The transitions are located between two age points – 27.48 and 23.53 ka BP (Wassenburg et al., 2012). Samples from the low-Mg aragonite layers were not analysed as the Mg content of aragonite is too low. The calcite layer yields $\delta^{26}\text{Mg}$ -values between $-4.29 \pm 0.02\%$ and $-3.89 \pm 0.06\%$ (mean: $-4.17 \pm 0.05\%$; Figs. 2 and 8a, Tables 2 and 3). Overall, $\delta^{26}\text{Mg}_{\text{calcite}}$ increase towards the overlying aragonite intervals, whilst isotope ratios remain invariant in the central portions of the calcite interval (Fig. 8a).

4.6 Flowstones SPA 52 and SPA 59, Spannagel Cave, Austria

The Pleistocene flowstones SPA 52 and SPA 59 $\delta^{26}\text{Mg}$ values show ranges from $-3.63 \pm 0.05\%$ to $-1.42 \pm 0.04\%$ (mean $-3.00 \pm 0.73\%$) and from $-4.06 \pm 0.04\%$ to $-2.47 \pm 0.05\%$ (mean: $-3.70 \pm 0.43\%$; Figs. 2, 9a and 10a, Tables 2 and 3), respectively. The highest $\delta^{26}\text{Mg}$ value for SPA 52 is located at 0.7 cm distance from base (dfb) in a detrital layer followed by a depleted $\delta^{26}\text{Mg}$ value at 7.0 cm dfb (Fig. 9a). Between 7.0 and 9.1 cm dfb the values slightly increase again. At 10.3 cm dfb the $\delta^{26}\text{Mg}$

The magnesium isotope record of cave carbonate archives

S. Riechelmann et al.

[Title Page](#)[Abstract](#)[Introduction](#)[Conclusions](#)[References](#)[Tables](#)[Figures](#)[⏪](#)[⏩](#)[◀](#)[▶](#)[Back](#)[Close](#)[Full Screen / Esc](#)[Printer-friendly Version](#)[Interactive Discussion](#)

is slightly depleted. The sample at 13.2 cm dfb is higher in its $\delta^{26}\text{Mg}$ and is located in a calcite layer containing slight amounts of detritus. After a hiatus of ca. 53 ka the $\delta^{26}\text{Mg}$ values are again higher (at 14.4 cm dfb) and are again lower at 16.7 cm dfb (Fig. 9a). These two sample points coincide with detrital layers.

Between 25.4 to 33.6 mm distance from base (dfb) the $\delta^{26}\text{Mg}$ values of SPA 59 are low before the $\delta^{26}\text{Mg}$ is higher at 41.1 mm dfb (Fig. 10a). This sample was taken at a hiatus with detrital material at the top. At 56.4 mm dfb the value is ^{26}Mg -depleted before the highest value is reached at 60.3 mm dfb ($\delta^{26}\text{Mg}$: -2.47% ; Fig. 10a). Samples taken at 47.5 and 60.3 mm dfb contain detrital material. Afterwards, the $\delta^{26}\text{Mg}$ values are again depleted 65.7 mm dfb and show a decreasing trend to 80.5 mm dfb. A slight increase occurs between 80.5 and 94.2 mm dfb followed by a decrease to 110.9 mm dfb (Fig. 10a).

5 Interpretation and discussion

The study sites are grouped into the following present-day climate regions (i) warm temperate and semi-arid (dry and hot summers) to arid (desert and hot arid) climate in Morocco; (ii) warm temperate (warm summers) and humid climate in Western Germany; (iii) equatorial-humid climate in Peru and (iv) alpine climate (humid, snow-rich winters and cold summers) in Austria (Kottek et al., 2006). Given that most of the following factors directly relate to climate, the discussion of Mg-isotope data is organized according to climate zones.

5.1 Environmental, equilibrium and non-equilibrium factors affecting the $\delta^{26}\text{Mg}$ -isotope fractionation in continental karst systems

Environmental, equilibrium and non-equilibrium factors affecting Mg isotope fractionation in Earth surface systems have been described in Galy et al. (2002), Young and Galy (2004), de Villiers et al. (2005), Tipper et al. (2006b, 2008, 2010), Buhl

CPD

8, 1835–1883, 2012

The magnesium isotope record of cave carbonate archives

S. Riechelmann et al.

Title Page

Abstract

Introduction

Conclusions

References

Tables

Figures

⏪

⏩

◀

▶

Back

Close

Full Screen / Esc

Printer-friendly Version

Interactive Discussion



et al. (2007), Brenot et al. (2008), Immenhauser et al. (2010), Pokrovsky et al. (2011) and Riechelmann et al. (2012b). Considering the published work, the following parameters are of significance for the interpretation of speleothem time-series $\delta^{26}\text{Mg}$ isotope data: (i) $\delta^{26}\text{Mg}$ signature of all involved Mg sources – rain water, soil cover (silicates) and hostrock (limestone or dolostone); (ii) the biogenic activity of the soil zone controlled mainly by water availability and air temperature; (iii) the balance between the silicate (Mg-bearing clay minerals) and carbonate weathering ratio in the soil zone, with clays being ^{26}Mg -enriched and diagenetically stabilized low Mg-calcite limestones being ^{26}Mg -depleted; (iv) the residence time of soil and karst water in the aquifer above the cave and (v) carbonate precipitation rates in the cave environment.

In contrast, even when considering the maximum range of Pleistocene to recent air temperature change in caves in Germany (ca. 9 to 10 °C; Richter et al., 2011), temperature-related $\delta^{26}\text{Mg}$ fractionation during calcite precipitation is a minor factor with experimental data suggesting a $\delta^{26}\text{Mg}$ dependency of 0.011 ‰ per °C from 4 to 45 °C (Li et al., 2012) and 0.02 ‰/AMU °C between 4 and 18 °C (Galy et al., 2002).

Rain water is ^{26}Mg -enriched with increasing distance to the marine aerosol source and may reveal temperature-related fractionation patterns, i.e. snow is ^{26}Mg depleted compared to rain (Tipper et al., 2010; Riechelmann et al., 2012b) but the existing data set is perhaps too limited to draw solid conclusions. The $\delta^{26}\text{Mg}$ ratio of dolostone (–2.2 to –1.1 ‰; Li et al., 2012) is in general higher than that of limestone (–5.3 to –1 ‰; Li et al., 2012), whilst silicate rocks and clay minerals have the most ^{26}Mg -enriched composition (–1.1 to +0.1 ‰; Immenhauser et al., 2010). Biological Mg fractionation by plants and soil microorganisms affect the Mg-isotope composition of the soil water in variable degrees depending on the amount of Mg involved and plant and microbial metabolisms (Tipper et al., 2010; Riechelmann et al., 2012b). Clearly, under warmer and wetter conditions soil activity is increased (Harper et al., 2005) and enhanced plant growth induces a stronger biological fractionation. Grass, for example, is ^{26}Mg -enriched in comparison with its rain water source (Tipper et al., 2010). Silicate (Mg-bearing clay minerals) weathering is relatively increasing during warmer and drier climate conditions

The magnesium isotope record of cave carbonate archives

S. Riechelmann et al.

[Title Page](#)[Abstract](#)[Introduction](#)[Conclusions](#)[References](#)[Tables](#)[Figures](#)[⏪](#)[⏩](#)[◀](#)[▶](#)[Back](#)[Close](#)[Full Screen / Esc](#)[Printer-friendly Version](#)[Interactive Discussion](#)

compared to carbonate weathering, which is always dominant but particularly so under more humid and cooler conditions (Buhl et al., 2007; Immenhauser et al., 2010).

Longer water residence times in the karst aquifer lead to lower $\delta^{26}\text{Mg}$ values in the drip waters, because the mixing time between younger, newly infiltrating ^{26}Mg -enriched water and older ^{26}Mg -depleted aquifer water is longer and hence leading to a bigger portion of the ^{26}Mg -depleted water. For shorter water residence times it is the opposite (Riechelmann et al., 2012b). Based on laboratory precipitation experiments (Immenhauser et al., 2010), lower carbonate precipitation rates lead to decreasing $\delta^{26}\text{Mg}$ values and vice versa. This, however, refers to experimental fluids that are considerably more saturated than those commonly found in cave environments and to precipitation rates (50 to 630 $\mu\text{mol h}^{-1}$) that exceed those of most natural speleothems (range of 0.0008 to 9.94 $\mu\text{mol h}^{-1}$ /0.1 to 1140 $\mu\text{m yr}^{-1}$ for AH-1, BU 4, NC-A, NC-B, SPA 52 and SPA 59). A statistically significant impact of experimental precipitation rate on calcite $\delta^{26}\text{Mg}$ is found at rates exceeding 200 $\mu\text{mol h}^{-1}$. Therefore, the direct applicability of the precipitation experiment data shown in Immenhauser et al. (2010) to natural systems is at present unclear.

5.2 Warm-(semi-)arid climate: speleothem time series $\delta^{26}\text{Mg}$ data from Morocco

Factors affecting weathering rates in carbonate-silicate settings are complex, spatially diverse and debated in the literature (Tipper et al., 2006a; Li et al., 2010; Pokrovsky et al., 2011). Nevertheless, rain water abundance and residence time in the soil as well as biogenic soil activity are considered significant (Tipper et al., 2006a, 2010; Li et al., 2010). Related to these factors, changes in the soil clay mineral to host limestone weathering balance affect the soil and aquifer water $\delta^{26}\text{Mg}$ value. Following the above discussion, a relative increase in the weathering of soil clay minerals induces higher $\delta^{26}\text{Mg}$ values. Under most hydrogeochemical conditions, the limestone and dolostone solubility in soil water and aquifer waters exceeds that of clay minerals (Appelo and Postma, 2005). Nevertheless, even a slightly increased solubility of Mg-bearing clay minerals will be recorded in soil-zone and karst aquifer waters due to

CPD

8, 1835–1883, 2012

The magnesium isotope record of cave carbonate archives

S. Riechelmann et al.

Title Page

Abstract

Introduction

Conclusions

References

Tables

Figures

⏪

⏩

◀

▶

Back

Close

Full Screen / Esc

Printer-friendly Version

Interactive Discussion



their high Mg-content and higher $\delta^{26}\text{Mg}$ values (Riechelmann et al., 2012b). Where dolostones or dolomite-rich limestones form the cave hostrock, the impact of silicate-derived ^{26}Mg on water isotope ratios will be subdued (Galy et al., 2002) due to the Mg-rich hostrock mineralogy.

The Moroccan stalagmite HK3, characterized by alternating aragonitic and calcitic intervals, documents the above relationships (Fig. 8). Due to the low abundance of Mg in aragonite (Okrusch and Matthes, 2005), sampling was restricted to the calcite intervals. Based on high-resolution carbon and oxygen isotope data as well as elemental abundances, Wassenburg et al. (2012) documented that during more arid periods, aragonite precipitation was favoured whilst calcite layers typify less arid conditions. During more arid phases, two main factors trigger aragonite precipitation. These include (i) the increased residence time of water in the soil as well as in the karst system, where ^{26}Mg enriched clays are leached, and (ii) prior calcite precipitation, which takes place in the karst aquifer zone (i.e. the precipitation of calcite prior to reaching the stalagmite surface), leading to a higher Mg-content of the fluid. The fact that the hostrock contains dolomite (Table 1) results in an enriched Mg-content of the drip water, too. In addition, prior calcite precipitation also increases the pH of the fluid and lowers the fluid saturation state. These factors give rise to aragonite precipitation (Frisia and Borsato, 2010; Wassenburg et al., 2012).

We used the stalagmite HK3 Mg-isotope data to test the above-described impact of increasing aridity and soil water residence time on the Mg-isotope signature. In essence, rainfall amount predictably decreases towards the calcite-to-aragonite transition (27.48 to 23.53 ka BP), whilst soil water residence time and silicate weathering rates in the aquifer should increase. Under increased input of isotopically more positive, clay-derived Mg a shift towards higher values near the calcite-to-aragonite transition is expected. Indeed, this shift in isotope ratios in the calcite layer near the transition to aragonite ($\Delta^{26}\text{Mg}=0.36\text{‰}$) is observed and documented in Fig. 8a. Carbon, oxygen and magnesium isotopes show a highly similar trend in the calcite layer (Fig. 8). However, it should be noticed that near the calcite-to-aragonite transition the possibility of

The magnesium isotope record of cave carbonate archives

S. Riechelmann et al.

[Title Page](#)[Abstract](#)[Introduction](#)[Conclusions](#)[References](#)[Tables](#)[Figures](#)[⏪](#)[⏩](#)[◀](#)[▶](#)[Back](#)[Close](#)[Full Screen / Esc](#)[Printer-friendly Version](#)[Interactive Discussion](#)

a mixing of predominantly calcite with small amounts of aragonite is found. Since the fractionation of carbon and oxygen isotopes is different for aragonite and calcite (Romanek et al., 1992; Kim and O'Neil, 1997), it may be possible that different fractionation factors also apply for Mg. Therefore, changes in the Mg-isotope composition near the calcite-to-aragonite transition may also be induced by a change of the fractionation factor.

The Mg-isotope record of the calcitic stalagmite GDA from Grotte d'Aoufous is equally well understood in the context of aridity changes. The Mg-isotope data (Fig. 7a) were thought to reflect changes between more or less arid conditions, which were in accordance with $\delta^{18}\text{O}$, $\delta^{13}\text{C}$, Sr and Mg elemental data and Sr isotopes (Buhl et al., 2007). Similar to the Moroccan stalagmite HK3, the $\delta^{26}\text{Mg}$ values of the GDA show a similar pattern as the $\delta^{13}\text{C}$ and $\delta^{18}\text{O}$ values (Fig. 7). Problems arise because stalagmite GDA is considerably older (U-Pb age of $2.134 \pm 0.115\text{Ma}$) and speleothem growth in the Grotte d'Aoufous ceased several times in the Pleistocene (Buhl et al., 2007). Climate reconstructions from Larrasoaña et al. (2003) and Feddi et al. (2011), however, support the interpretation of stalagmite GDA from Buhl et al. (2007). For the Gelasian (1.806–2.588 Ma), i.e. the time interval that coincides with the U-Pb age of stalagmite GDA, Larrasoaña et al. (2003) found changes in the dust amount, interpreted as changes in the amount of rainfall that coincides with changes of the 400-kyr component of the eccentricity. According to these authors, changes between more arid and less arid conditions occur during the Gelasian. Similarly, Feddi et al. (2011) documented evidence for temperature changes in the Gelasian from pollen analyses. These general patterns are arguably also recorded in stalagmite GDA, which is therefore showing changes between more arid and warm and less arid and warm conditions in the Mg-isotope composition.

The hostrock $\delta^{26}\text{Mg}$ of Grotte d'Aoufous ($-3.63 \pm 0.08\%$; Fig. 2; Buhl et al., 2007), a Turonian marine limestone, is slightly higher than that of the Devonian hostrock ($-3.72 \pm 0.07\%$; Fig. 2; Immenhauser et al., 2010) values of the caves in Germany discussed below. Aquifer water residence time under the arid conditions that characterize

The magnesium isotope record of cave carbonate archives

S. Riechelmann et al.

Title Page

Abstract

Introduction

Conclusions

References

Tables

Figures

⏪

⏩

◀

▶

Back

Close

Full Screen / Esc

Printer-friendly Version

Interactive Discussion

the northern rim of the Sahara were expectedly longer than those in the warm-humid climate in Germany. Hence, lower $\delta^{26}\text{Mg}$ values for the Moroccan stalagmite GDA could be expected.

In essence, the concepts as explained above provide a comparably robust and internally consistent interpretation for the $\delta^{26}\text{Mg}$ record of the two Moroccan speleothems shown here. Combined with evidence from Sr and Mg abundances and calcite $^{87}\text{Sr}/^{86}\text{Sr}$ ratios – i.e. more radiogenic $^{87}\text{Sr}/^{86}\text{Sr}$ under more arid conditions due to longer siliceous rock/water interaction (Buhl et al., 2007) – it is proposed that shifts towards lower $\delta^{26}\text{Mg}$, $\delta^{13}\text{C}$ and $\delta^{18}\text{O}$ values (Figs. 7 and 8) represent less arid and perhaps lower temperatures whilst higher isotope ratios point to more arid and hot desert climate (Fig. 11). The above considerations suggest that speleothem Mg isotope data from warm-(semi-)arid settings are useful and sensitive proxies for climate driven changes in the carbonate-silicate weathering balance.

5.3 Equatorial-humid climate: speleothem time series $\delta^{26}\text{Mg}$ data from Peru

The Holocene climate in Peru differs significantly from that of the Moroccan case examples. The present-day rainfall amount in the vicinity of the Cueva del Tigre Perdido is around 1344 mm yr^{-1} (Table 1; Sträßer, 1999); and was probably in the order of $940\text{--}1140\text{ mm yr}^{-1}$ at the beginning of the Holocene (15–30 % increase of rainfall amount during the Holocene; van Breukelen et al., 2008), a value that indicates an overall very humid climate. Average annual temperatures seem to have remained rather constant through the Holocene (van Breukelen et al., 2008). This overall pattern is documented in the $\delta^{18}\text{O}_{\text{calcite}}$ data that decrease during the Holocene due to a gradual increase of rainfall amount (van Breukelen et al., 2008). It seems likely, that water residence times were short due to the high and constantly high rainfall amount at this site. Therefore, no changes in the Mg-isotope values should be expected.

In contrast to the Moroccan case examples, the Peruvian stalagmites NC-A and NC-B lack a correlation between $\delta^{26}\text{Mg}$ and $\delta^{13}\text{C}$ and $\delta^{18}\text{O}$ ratios, respectively (Fig. 6). Applying the concepts laid out above, the limited changes in the (short) soil water

The magnesium isotope record of cave carbonate archives

S. Riechelmann et al.

Title Page

Abstract

Introduction

Conclusions

References

Tables

Figures

⏪

⏩

◀

▶

Back

Close

Full Screen / Esc

Printer-friendly Version

Interactive Discussion



residence and a rather constant carbonate versus silicate weathering ratio throughout the Late Pleistocene to Late Holocene – the soil is mainly composed of kaolinite and Mg-bearing montmorillonite (Sanchez and Buol, 1974) – resulted in invariant $\delta^{26}\text{Mg}$ ratios in stalagmite NC-B (Fig. 6a). In contrast, the Late Holocene to recent NC-A speleothem recorded subtle changes in $\delta^{26}\text{Mg}_{\text{calcite}}$ barely exceeding the analytical error that are not reflected in the C or O isotope ratios. Considering the limitations of the low temporal resolution of $\delta^{26}\text{Mg}$ sampling points and the invariant Mg-isotope signatures, it is here proposed that the Peruvian stalagmites represent an end-member case setting that is less than suitable for Mg isotope proxy data.

5.4 Warm-humid climate: speleothem time series $\delta^{26}\text{Mg}$ data from Germany

Figure 4 documents all $\delta^{26}\text{Mg}$ values of stalagmite AH-1 from samples that were crushed prior to analysis and that are isotopically depleted relative to aliquots of the same sample that have not been treated in this manner. The trend in Mg-isotopes with time is the same for the crushed samples and the bulk samples (Fig. 4). From this it is concluded, that the $\delta^{26}\text{Mg}$ of the fluid contained in these inclusions shifts the bulk calcite Mg-isotope composition by 0.01 to 0.08‰ towards higher values. This is because the fluid representing the drip water chemistry – enriched in $\delta^{26}\text{Mg}$ relative to the calcite (Galy et al., 2002; Young and Galy, 2004; Immenhauser et al., 2010; Riechelmann et al., 2012) – is influenced by the same factors as the calcite that has precipitated from this fluid (Riechelmann et al., 2012b).

The interpretation of speleothem $\delta^{26}\text{Mg}$ time series data from Atta and Bunker Caves is challenging. Given the very comparable climate setting, hostrock composition ($\delta^{26}\text{Mg}$: $-3.72 \pm 0.07\%$; Fig. 2; Immenhauser et al., 2010) and soil properties, we suggest that the same set of factors drive Mg fractionation in these two caves. Differences between the two sites include drip characteristics as well as drip water chemistry.

Both drip sites show only slight differences in their drip rate (AH-1: $0.019 \pm 0.001 \text{ ml min}^{-1}$; Niggemann, 2000; BU 4: $0.002 \pm 0.001 \text{ ml min}^{-1}$) but the same drip characteristic (seepage flow) using the terminology of Baker et al. (1997). The fact, that the

CPD

8, 1835–1883, 2012

The magnesium isotope record of cave carbonate archives

S. Riechelmann et al.

Title Page

Abstract

Introduction

Conclusions

References

Tables

Figures

⏪

⏩

◀

▶

Back

Close

Full Screen / Esc

Printer-friendly Version

Interactive Discussion



drip rate of the AH-1 drip site is ten times faster than that of the BU 4 drip site probably suggests that the water feeding the AH-1 drip site (Atta Cave) has a shorter water residence time compared to that of the BU 4 drip site (Bunker Cave). This assumption is supported by field evidence given that speleothem BU 4 is characterized by a lower mean $\delta^{26}\text{Mg}$ value ($-4.20 \pm 0.10\text{‰}$; Fig. 2 and Table 3) compared to speleothem AH-1 ($-4.01 \pm 0.07\text{‰}$, Fig. 2 and Table 3). This because the aquifer water in Bunker Cave has a longer reaction time with the isotopically depleted hostrock in the karst zone.

Nevertheless, differences in drip water chemistry might also be the reason for the differences in mean Mg-isotope composition of 0.19‰ between these two caves. Drip water samples taken above AH-1 is considerably enriched in Mg (Mg/Ca ratio: 0.67; Niggemann, 2000) relative to drip water samples taken above BU 4 (Mg/Ca ratio: 0.06). Higher Mg concentrations in the aquifer may be due to dolomitisation of the limestone along fissures in the hostrock (Krebs, 1978). Water feeding the drip site of AH-1 is possibly percolating along these dolomitized fissures. This seems not to be the case for the drip water of BU 4. Given that dolomite is generally elevated in $\delta^{26}\text{Mg}$ relative to limestone (Li et al., 2012), higher mean $\delta^{26}\text{Mg}$ value of AH-1 drip water are expected and found.

The portion of stalagmite AH-1 representing the time interval between 9.0 to 6.0 ka BP is characterized by a dark and compact crystal fabric. Calcite precipitated between 6 ka BP and Present is typified by a white and porous crystal fabric. Lower $\delta^{26}\text{Mg}$ values correspond with the dark and compact crystal fabric and ^{26}Mg -enriched values correspond with the white and porous crystal fabric.

In AH-1, carbon and oxygen isotope values (Fig. 3b) are enriched in the dark, dense fabric (9.0 to 6.0 ka BP), a fact that was interpreted as evidence for overall drier climate conditions (Niggemann et al., 2003). As argued in Riechelmann et al. (2012b), drier climate in essence shifts the silicate versus carbonate weathering ratio towards isotopically less depleted (silicate) values. Higher $\delta^{26}\text{Mg}$ values would be expected rather than lower values as observed. Between 6.0 and the present day, the climate was overall wetter (Niggemann et al., 2003) and ^{26}Mg -enriched values are found as opposed

The magnesium isotope record of cave carbonate archives

S. Riechelmann et al.

[Title Page](#)[Abstract](#)[Introduction](#)[Conclusions](#)[References](#)[Tables](#)[Figures](#)[⏪](#)[⏩](#)[◀](#)[▶](#)[Back](#)[Close](#)[Full Screen / Esc](#)[Printer-friendly Version](#)[Interactive Discussion](#)

to ^{26}Mg -depleted values as expected for dominant carbonate weathering under wetter conditions. Based on the $\delta^{18}\text{O}$ record of stalagmite AH-1, Mangini et al. (2007) proposed an overall climatic warming for the last 6 ka BP.

The following lines of evidence (Riechelmann et al., 2012b) suggest that under an overall humid climate and increasing mean air temperature microbial soil-zone activity is favoured (Harper et al., 2005). Related to this, the weathering of Mg-bearing clay minerals such as montmorillonite, chlorite and illite in the soil zone is increased. The general shift in $\delta^{26}\text{Mg}_{\text{AH-1}}$ towards higher values may bear witness of an overall increased influx of clay-derived ^{26}Mg . If these considerations hold true, the general trend in AH-1 $\delta^{26}\text{Mg}$ is mainly outside air temperature controlled. Between 9 to 6 ka BP carbonate weathering increased relative to clay mineral weathering in the soil zone due to colder temperatures. Between 6 ka BP to Present, a renewed increase in outside air temperature favoured silicate weathering in the soil zone (Figs. 3a and 11).

Using oxygen isotope data of AH-1 (Niggemann, 2000; Niggemann et al., 2003) as a tentative benchmark against which the smaller variations in $\delta^{26}\text{Mg}$ are calibrated, the following pattern emerges: Shifts towards higher $\delta^{26}\text{Mg}$ values took place when mean rainfall amounts decreased whilst shifts towards lower $\delta^{26}\text{Mg}$ values coincided with overall more humid climate (Figs. 3 and 11).

The stalagmite BU 4 consists of a columnar fabric with the exception of a thin interval dated as 7.6 ka BP that is characterized by dendritic crystals (Riechelmann, 2010). It is of interest to note that $\delta^{26}\text{Mg}$ ratios shift to higher values at this level (Fig. 5a) but the relation between crystallography and Mg isotope ratios is still underexplored. Columnar crystal fabrics are formed under stable precipitation conditions, while dendritic fabric forms preferentially under conditions far from equilibrium (Frisia et al., 2000; Frisia and Borsato, 2010).

Following Fohlmeister et al. (2012), $\delta^{18}\text{O}$ data of BU 4 recorded changes in both temperature and rainfall amount – at higher values the climate was cooler and drier and vice versa (Fig. 5b). The first order signal of $\delta^{13}\text{C}$ is influenced by vegetation cover above the cave while the second order signal is influenced by drip rate (Fohlmeister

The magnesium isotope record of cave carbonate archives

S. Riechelmann et al.

Title Page

Abstract

Introduction

Conclusions

References

Tables

Figures

⏪

⏩

◀

▶

Back

Close

Full Screen / Esc

Printer-friendly Version

Interactive Discussion



et al., 2012). Between 9 to 7 ka BP soil respiration was lower leading to higher $\delta^{13}\text{C}$ values. After 7 ka BP the $\delta^{13}\text{C}$ signal decreases, which is due to a denser vegetation cover and thus higher soil respiration (Fohlmeister et al., 2012). Periods of lower drip rate lead to higher $\delta^{13}\text{C}$ values and vice versa (Fohlmeister et al., 2012).

Between 8.2 and 6.0 ka BP, the $\delta^{13}\text{C}$ and $\delta^{18}\text{O}$ data of BU 4 indicate a trend to drier and cooler climate with less soil respiration (Fig. 5b), whilst the Mg-isotope values decrease (Fig. 5a). Following our previous set of arguments, this points to a shift towards carbonate weathering with temperature overruling rainfall amount as the driving factor (Fig. 11).

From 5.5 to 1.8 ka BP, $\delta^{13}\text{C}$ and $\delta^{26}\text{Mg}$ values both show a decreasing trend (Fig. 5). Soil respiration expectedly increased during this time due to the development of a denser vegetation cover (Fohlmeister et al., 2012). Hence, the production of CO_2 is increased and leads to higher dissolution rates of the low-Mg calcite hostrock due to the increased amount of carbonic acid in the karst system. Also the decalcification of the loess (at present a loess loam) may have lead to decreasing $\delta^{26}\text{Mg}$ values. Therefore, decreasing $\delta^{26}\text{Mg}$ values may be due to enhanced dissolution of carbonate between 5.5 to 1.8 ka BP. The processes might also apply between 5.7 and 4.2 ka BP for speleothem AH-1. Here, a decreasing trend in the $\delta^{26}\text{Mg}$ is noted (Fig. 3a), whilst $\delta^{13}\text{C}$ values decrease but to a lesser degree (Fig. 3b). The direct comparison of the Bunker Cave stalagmites $\delta^{18}\text{O}$ record with that of the Atta Cave stalagmite AH-1 reveals similar patterns (Fohlmeister et al., 2012). This observation is considered evidence that stalagmites in both caves recorded essentially the same environmental signals.

BU 4 magnesium-isotope ratios between 1.6 and 0.7 ka BP anti-correlate with BU 4 $\delta^{13}\text{C}$ and $\delta^{18}\text{O}$ data (Fig. 5). As a consequence, it seems that temperature is again the factor dominating soil processes and linked to this, weathering ratios (Fig. 11). Between 1.1 to 0.7 ka, the Medieval Warm Period (Fohlmeister et al., 2012) is characterized by lower $\delta^{13}\text{C}$ and $\delta^{18}\text{O}$ and higher $\delta^{26}\text{Mg}$ values (Fig. 5), perhaps explained by an overall

The magnesium isotope record of cave carbonate archives

S. Riechelmann et al.

Title Page

Abstract

Introduction

Conclusions

References

Tables

Figures

⏪

⏩

◀

▶

Back

Close

Full Screen / Esc

Printer-friendly Version

Interactive Discussion

wetter and warmer climate (Esper et al., 2002; Soon et al., 2003; Negendank, 2004; Mann et al., 2009).

The Little Ice Age, dated between 0.7 to 0.2 ka, is characterized by a shift to higher values in $\delta^{13}\text{C}$ and $\delta^{18}\text{O}$ and lower $\delta^{26}\text{Mg}$ ratios (Fig. 5; Fohlmeister et al., 2012) indicating overall drier and cooler climate (Esper et al., 2002; Soon et al., 2003; Negendank, 2004; Mann et al., 2009). Published mean air temperature differences from Western Germany between Little Ice Age and Medieval Warm Period are on the order of 2 to 2.5 °C (Negendank, 2004). Given the low dependency of Mg isotope fractionation on temperature during calcite precipitation (0.02 ‰/AMU/°C; Galy et al., 2002), the observed isotope shifts would require cave temperature changes in excess of 10 °C. Evidence for a temperature shift in this order of magnitude is lacking and temperature is thus ruled out as a main factor driving Mg isotope fractionation during calcite precipitation.

High $\delta^{26}\text{Mg}$ values in BU 4 coincide with a hiatus at 5.5 ka BP containing detrital material (Fig. 5a) as does one sample taken from stalagmite AH-1 at 7.9 ka BP (Fig. 3a). Besides quartz, feldspar and mica, detrital layers contain high amounts of clay minerals that are in part dissolved in 6M HCl especially during heating (Madejová et al., 1998; Komadel and Madejová, 2006). It seems thus likely that clay mineral-derived, isotopically heavy magnesium is analysed in parallel with the calcite-derived magnesium (Figs. 3a and 5a). In essence, the two cave records from Germany exemplify the full complexity of speleothem $\delta^{26}\text{Mg}$ records in a setting characterized by comparably subtle climate changes over time. Based on the arguments brought forward here, it is suggested that weathering patterns in the soil zone above the caves as well as in the karst zone, driven by mean outside air temperature and rainfall amount, are the main driving factors in the $\delta^{26}\text{Mg}$ records obtained (Fig. 11). In principle, all of these factors are present at all times but temperature seems to overrule rainfall amount in general.

The magnesium isotope record of cave carbonate archives

S. Riechelmann et al.

Title Page

Abstract

Introduction

Conclusions

References

Tables

Figures

⏪

⏩

◀

▶

Back

Close

Full Screen / Esc

Printer-friendly Version

Interactive Discussion



5.5 Cold-humid climate: speleothem time series $\delta^{26}\text{Mg}$ data from Austria

Speleothem deposition in the high-elevation Spannagel Cave is biased towards warm interglacial conditions. Cold-climate precipitation, however, has also been observed and attributed to the presence of sulphides in the hostrock (providing acidity for karstification) and a warm-based ice cover (Spötl et al., 2007; Spötl and Mangini, 2007). In the present-day setting, sparse alpine meadows cover a soil above the cave and soil thickness does not exceed 20 cm. Portions of the hostrock above the cave are bare, meaning not covered by soil or vegetation.

Carbon isotope ratios of both studied flowstones (Figs. 9b and 10b) are influenced by the composition of the marine marble hostrock ($\delta^{13}\text{C}$ of +2 to +3‰; Holzkämper et al., 2005) and the input of soil-derived organic C in the drip water. Oxygen isotope values are high during warm and low during cold climate conditions. Low $\delta^{13}\text{C}$ values imply more biological activity in the soil zone and vice versa (Spötl et al., 2007; Holzkämper et al., 2005). Decreasing $\delta^{13}\text{C}$ values thus reflect a genuine vegetation signal during periods, when carbon is anti-correlated with oxygen (Spötl et al., 2007; Holzkämper et al., 2005).

Both flowstones show similar patterns in $\delta^{26}\text{Mg}$ and $\delta^{18}\text{O}$ (Figs. 9 and 10). Higher values during warm conditions may thus imply more silicate weathering and vice versa. During interglacials the availability of water (rain, snow and ice melt) is higher than during glacial periods (Spötl et al., 2007). Hence, changes in rainfall amount that in turn affect soil activity can be excluded as main factor controlling Mg-isotope fractionation, because speleothems can not form without water availability. Having ruled out water availability as a controlling factor, temperature remains the main parameter controlling subtle changes in silicate versus carbonate weathering ratios (Fig. 11). This probably applies for the Holocene with warm summer months and cold winter months (7 to 8 months of snow cover per year; Spötl et al., 2002).

Flowstones yield numerous detrital layers, which were sampled (red triangles in Figs. 9 and 10). As found in the case of BU 4 and AH-1, Mg-bearing clay minerals

The magnesium isotope record of cave carbonate archives

S. Riechelmann et al.

Title Page

Abstract

Introduction

Conclusions

References

Tables

Figures

⏪

⏩

◀

▶

Back

Close

Full Screen / Esc

Printer-friendly Version

Interactive Discussion

were also partly dissolved during sample preparation and shift the Mg-isotope ratios towards higher values. Sample SPA 52 f ($\delta^{26}\text{Mg}$: $-1.42 \pm 0.04\%$; Table 2) and sample SPA 59 b ($\delta^{26}\text{Mg}$: $-2.47 \pm 0.05\%$; Table 2) are taken from thick detrital layers with a high clay mineral content and are therefore highly ^{26}Mg -enriched. Given that these data points are not representing the calcite $\delta^{26}\text{Mg}$ ratios, mean values should be calculated without samples containing detritus (new mean $\delta^{26}\text{Mg}$ SPA 52: $-3.48 \pm 0.15\%$; new mean $\delta^{26}\text{Mg}$ SPA 59: $-3.88 \pm 0.12\%$).

Flowstone SPA 52 is characterized by considerably elevated mean $\delta^{26}\text{Mg}$ values of -3.48% relative to flowstone SPA 59 ($\delta^{26}\text{Mg}$: -3.88%). This may indicate that the drip water feeding SPA 59 experienced an overall longer residence time. Furthermore, the hostrock $\delta^{26}\text{Mg}$ ratio is $-3.23 \pm 0.24\%$ (Fig. 2) and therefore closer to the mean isotopic composition of SPA 52 relative to SPA 59, a feature that is in good agreement with a short hostrock water residence time.

In conclusion, the Spannagel flowstones represent a cold, alpine endmember setting characterized by mainly temperature-driven weathering changes in the thin soil cover – where present – above the cave (Fig. 11). Warmer periods favour more soil-zone activity and increased silicate weathering leading to enriched $\delta^{26}\text{Mg}$.

5.6 Potential, problems and future work

Data shown here suggest that a limited, albeit complicated bundle of parameters controls the Mg isotope composition of speleothems. Here, we show data from a series of climatic zones. Obviously, caves situated in climate domains characterized by pronounced changes in mean air temperature or rainwater availability are expectedly characterized by more pronounced shifts (Fig. 11). A prominent example is found in the data set from Morocco. Conversely, speleothem records characterized by rather constant climate parameters such as the Peruvian data, show no variability in $\delta^{26}\text{Mg}$.

The interpretation of the $\delta^{26}\text{Mg}$ records from caves in Germany are complex. This is because several of the factors, namely temperature and rainfall amount, control speleothem $\delta^{26}\text{Mg}$ in a manner that differs from the Moroccan stalagmites $\delta^{26}\text{Mg}$.

In the cold, alpine end member, outside air temperature seems the dominant driver of carbonate-silicate weathering patterns driving the $\delta^{26}\text{Mg}$ variations.

One of the obvious strengths of the Mg isotope proxy is its sensitivity for subtle processes in the soil zone (weathering ratios; Buhl et al., 2007) and differences in soil and reservoir water residence time (Riechelmann et al., 2012b). Combined with elemental evidence and other isotope systems such as Sr, C, and O, an improved understanding of soil zone processes can be achieved. Nevertheless, despite significant advances in the application of Mg-isotopes as a continental climate proxy, unsolved issues remain. Due to the low Mg content of many speleothems, the sample size required for $\delta^{26}\text{Mg}$ analysis is large and – combined with the time-consuming and expensive analytical work – inhibit high-resolution speleothem Mg isotope records similar to C or O isotopes. Specifically, aragonite speleothems are low in Mg so that an interpretation of their $\delta^{26}\text{Mg}$ records seems not feasible at present. Therefore, comparisons between high-resolution C, O and elemental data records with $\delta^{26}\text{Mg}$ data in speleothems are difficult at present. The sampling of speleothem calcite containing detrital material should be avoided due to contamination problems. The dependency of the $\delta^{26}\text{Mg}$ on the calcite precipitation rate is known from laboratory precipitation experiments (Immenhauser et al., 2010), but awaits further work using water compositions and precipitation rates that are more similar to those found in nature, since there was no influence on $\delta^{26}\text{Mg}$ in natural samples observed.

Finally, an improved understanding of the factors that control Mg leaching from soil zone clay minerals and clay contained in hostrock carbonates is required. Carefully established leaching experiments under controlled laboratory conditions might represent the way forward.

CPD

8, 1835–1883, 2012

The magnesium isotope record of cave carbonate archives

S. Riechelmann et al.

Title Page

Abstract

Introduction

Conclusions

References

Tables

Figures

⏪

⏩

◀

▶

Back

Close

Full Screen / Esc

Printer-friendly Version

Interactive Discussion

6 Conclusions

The analysis of Mg as well as C and O isotope ratios from eight speleothems representing five climate zones leads to the following conclusions:

1. The sensitivity of speleothem $\delta^{26}\text{Mg}$ values to environmental and kinetic factors strongly depends on the overall climate setting. Pronounced variations in mean air temperature and rainfall amount with time, such as the case in the Pleistocene of Morocco, result in changes in the silicate versus carbonate weathering ratio that in turn affects drip water $\delta^{26}\text{Mg}$ in a predictable manner. Caves situated in invariant climate domains, such as tropical Peru during the Pleistocene to Holocene, are characterized by invariant $\delta^{26}\text{Mg}$ records.
2. Stalagmite $\delta^{26}\text{Mg}$ values from warm-temperate climate zones such as Western Germany are more difficult to interpret. This is because factors interfere in a more complex manner. These factors include mean air temperature outside the cave and rainfall amount. These factors drive soil-zone activity and affect the subtle balance between silicate and carbonate weathering rates. Here, multi-proxy C and O data must be used in combination with $\delta^{26}\text{Mg}$ ratios in order to obtain a coherent interpretation and to separate the relative effects of mean air temperature and rainfall amount on soil zone activity.
3. Layers of detrital material in speleothems must be avoided due to contamination problems. Particularly, Mg-bearing clay minerals shift bulk values to higher $\delta^{26}\text{Mg}$ ratios.
4. In high-latitude and alpine climate settings exposed to pronounced changes in glacial and interglacial air temperature, the main driving factor of soil-zone activity and weathering ratios outside of the cave is temperature controlling weathering ratios and hence speleothem $\delta^{26}\text{Mg}$ values.

The magnesium isotope record of cave carbonate archives

S. Riechelmann et al.

Title Page

Abstract

Introduction

Conclusions

References

Tables

Figures

⏪

⏩

◀

▶

Back

Close

Full Screen / Esc

Printer-friendly Version

Interactive Discussion



The magnesium isotope record of cave carbonate archives

S. Riechelmann et al.

Title Page

Abstract

Introduction

Conclusions

References

Tables

Figures

⏪

⏩

◀

▶

Back

Close

Full Screen / Esc

Printer-friendly Version

Interactive Discussion

5. Comparing hostrock and mean $\delta^{26}\text{Mg}$ stalagmite signatures, semi-quantitative estimates of aquifer water residence time can be obtained. Depleted mean stalagmite $\delta^{26}\text{Mg}$ values are found where hostrock values are low and long residence time resulted in equilibration of $\delta^{26}\text{Mg}_{\text{fluid}}$ with $\delta^{26}\text{Mg}_{\text{hostrock}}$.

6. The results shown here summarize the present level of knowledge in speleothem Mg isotope proxy research. An improved understanding of the complex processes involved requires well calibrated experimental work including leaching and precipitation experiments.

Acknowledgements. We thank our colleagues in the non-traditional isotope laboratory at Bochum for technical assistance. The Speleogroup Letmathe is thanked for supporting sample recovery in Atta and Bunker Cave. Uranium-lead age dating of the Grotte d'Aoufous stalagmite in Morocco was performed at the University of Berne, Switzerland. This is a contribution to the collaborative research initiative DAPHNE II, founded by the DFG.

References

- Appelo, C. A. J. and Postma, D.: *Geochemistry, Groundwater and Pollution*, 2. Edn., A. A. Balkema Publishers, Amsterdam, 649 pp., 2005.
- Asrat, A., Baker, A., Leng, M. J., Gunn, J., and Umer, M.: Environmental monitoring in the Mechara caves, Southeastern Ethiopia: implications for speleothem palaeoclimate studies, *Int. J. Speleol.*, 37, 207–220, 2008.
- Baker, A. and Genty, D.: Environmental pressures on conserving cave speleothems: effects of changing surface land use and increased cave tourism, *J. Environ. Manage.*, 53, 165–175, 1998.
- Baker, A., Barnes, W. L., and Smart, P. L.: Variations in the discharge and organic matter content of stalagmite drip waters in Lower Cave, Bristol, *Hydrol. Process.*, 11, 1541–1555, 1997.

The magnesium isotope record of cave carbonate archives

S. Riechelmann et al.

[Title Page](#)[Abstract](#)[Introduction](#)[Conclusions](#)[References](#)[Tables](#)[Figures](#)[⏪](#)[⏩](#)[◀](#)[▶](#)[Back](#)[Close](#)[Full Screen / Esc](#)[Printer-friendly Version](#)[Interactive Discussion](#)

Baldini, J. U. L., McDermott, F., Hoffmann, D. L., Richards, D. A., and Clipson, N.: Very high-frequency and seasonal cave atmosphere P_{CO_2} variability: implications for stalagmite growth and oxygen isotope-based paleoclimate records, *Earth Planet. Sc. Lett.*, 272, 118–129, doi:10.1016/j.epsl.2008.04.031, 2008.

5 Brenot, A., Cloquet, C., Vigier, N., Carignan, J., and France-Lanord, C.: Magnesium isotope systematics of the lithologically varied Moselle river basin, France, *Geochim. Cosmochim. Acta*, 72, 5070–5089, doi:10.1016/j.gca.2008.07.027, 2008.

Buhl, D., Immenhauser, A., Smeulders, G., Kabiri, L., and Richter, D. K.: Time series $\delta^{26}\text{Mg}$ analysis in speleothem calcite: kinetic versus equilibrium fractionation, comparison with
10 other proxies and implications for palaeoclimate research, *Chem. Geol.*, 244, 715–729, doi:10.1016/j.chemgeo.2007.07.019, 2007.

Collister, C. and Matthey, D.: Controls on water drop volume at speleothem drip sites: an experimental study, *J. Hydrol.*, 358, 259–267, doi:10.1016/j.jhydrol.2008.06.008, 2008.

15 Cruz Jr., F. W., Burns, S. J., Jercinovic, M., Karmann, I., Sharp, W. D., and Vuille, M.: Evidence of rainfall variations in Southern Brazil from trace element ratios (Mg/Ca and Sr/Ca) in a Late Pleistocene stalagmite, *Geochim. Cosmochim. Acta*, 71, 2250–2263, doi:10.1016/j.gca.2007.02.005, 2007.

Daëron, M., Guo, W., Eiler, J., Genty, D., Blamart, D., Boch, R., Drysdale, R., Maire, R., Wainer, K., and Zanchetta, G.: $^{13}\text{C}^{18}\text{O}$ clumping in speleothems: observations from natural caves and precipitation experiments, *Geochim. Cosmochim. Acta*, 75, 3303–3317,
20 10.1016/j.gca.2010.10.032, 2011.

de Villiers, S., Dickson, J. A. D., and Ellam, R. M.: The composition of the continental river weathering flux deduced from seawater Mg isotopes, *Chem. Geol.*, 216, 133–142, doi:10.1016/j.chemgeo.2004.11.010, 2005.

25 DePaolo, D. J.: Surface kinetic model for isotopic and trace element fractionation during precipitation of calcite from aqueous solutions, *Geochim. Cosmochim. Acta*, 75, 1039–1056, 10.1016/j.gca.2010.11.020, 2011.

Dorale, J. A., Edwards, R. L., Ito, E., and González, L. A.: Climate and vegetation history of the midcontinent from 75 to 25 ka: a speleothem record from Crevice Cave, Missouri, USA, *Science*, 282, 1871–1874, 1998.

30 Dreybrodt, W. and Scholz, D.: Climatic dependence of stable carbon and oxygen isotope signals recorded in speleothems: from soil water to speleothem calcite, *Geochim. Cosmochim. Acta*, 75, 734–752, doi:10.1016/j.gca.2010.11.002, 2011.

The magnesium isotope record of cave carbonate archives

S. Riechelmann et al.

[Title Page](#)
[Abstract](#)
[Introduction](#)
[Conclusions](#)
[References](#)
[Tables](#)
[Figures](#)
[Back](#)
[Close](#)
[Full Screen / Esc](#)
[Printer-friendly Version](#)
[Interactive Discussion](#)


- Esper, J., Cook, E. R., and Schweingruber, F. H.: Low-frequency signals in long tree-ring chronologies for reconstructing past temperature variability, *Science*, 295, 2250–2253, 2002.
- Fairchild, I. J. and McMillan, E. A.: Speleothems as indicators of wet and dry periods, *Int. J. Speleol.*, 36, 69–74, 2007.
- 5 Feddi, N., Fauquette, S., and Suc, J.-P.: Histoire plio-pléistocène des écosytèmes végétaux de méditerranée sud-occidentale: apport de l'analyse pollinique de deux sondages en mer d'alboran, *GEOBIOS*, 44, 57–69, doi:10.1016/j.geobios.2010.03.007, 2011.
- Fohlmeister, J., Schröder-Ritzrau, A., Scholz, D., Spötl, C., Riechelmann, D. F. C., Mudelsee, M., Wackerbarth, A., Gerdes, A., Riechelmann, S., Immenhauser, A., Richter, D. K., and
10 Mangini, A.: Bunker Cave stalagmites: an archive for central European Holocene climate variability, *Clim. Past Discuss.*, 8, 1687–1720, doi:10.5194/cpd-8-1687-2012, 2012.
- Frisia, S. and Borsato, A.: Karst, in: *Carbonates in Continental Settings: Facies, Environments and Processes*, edited by: Alonso-Zarza, A. M. and Tanner, L. H., *Developments in Sedimentology*, Vol. 61, Elsevier, Amsterdam, 269–318, 2010.
- 15 Frisia, S., Borsato, A., Fairchild, I. J., and McDermott, F.: Calcite fabrics, growth mechanisms, and environments of formation in speleothems from the Italian Alps and Southwestern Ireland, *J. Sediment. Res.*, 70, 1183–1196, 2000.
- Frisia, S., Borsato, A., Fairchild, I. J., McDermott, F., and Selmo, E. M.: Aragonite-calcite relationships in speleothems (Grotte de Clamouse, France): environment, fabrics, and carbonate
20 geochemistry, *J. Sediment. Res.*, 72, 687–699, 2002.
- Galy, A., Bar-Matthews, M., Halicz, L., and O'Nions, R. K.: Mg isotopic composition of carbonate: insight from speleothem formation, *Earth Planet. Sc. Lett.*, 201, 105–115, 2002.
- Genty, D. and Massault, M.: Carbon transfer dynamics from bomb-¹⁴C and δ^{13} C time series of a laminated stalagmite from SW France – modelling and comparison with other stalagmite
25 records, *Geochim. Cosmochim. Acta*, 63, 1537–1548, 1999.
- Harper, C. W., Blair, J. M., Fay, P. A., Knapp, A. K., and Carlisle, J. D.: Increased rainfall variability and reduced rainfall amount decreases soil CO₂ flux in a grassland ecosystem, *Global Change Biol.*, 11, 322–334, doi:10.1111/j.1365–2486.2005.00899.x, 2005.
- Holzkaemper, S., Spötl, C., and Mangini, A.: High-precision constraints on timing of alpine warm periods during the middle to late Pleistocene using speleothem growth periods, *Earth Planet. Sc. Lett.*, 236, 751–764, doi:10.1016/j.epsl.2005.06.002, 2005.
- 30 Huang, Y. and Fairchild, I. J.: Partitioning of Sr²⁺ and Mg²⁺ into calcite under karst-analogue experimental conditions, *Geochim. Cosmochim. Acta*, 65, 47–62, 2001.

The magnesium isotope record of cave carbonate archives

S. Riechelmann et al.

[Title Page](#)
[Abstract](#)
[Introduction](#)
[Conclusions](#)
[References](#)
[Tables](#)
[Figures](#)




[Back](#)
[Close](#)
[Full Screen / Esc](#)
[Printer-friendly Version](#)
[Interactive Discussion](#)


- Immenhauser, A., Buhl, D., Richter, D. K., Niedermayr, A., Riechelmann, D., Dietzel, M., and Schulte, U.: Magnesium-isotope fractionation during low-Mg calcite precipitation in a limestone cave – field study and experiments, *Geochim. Cosmochim. Acta*, 74, 4346–4364, doi:10.1016/j.gca.2010.05.006, 2010.
- 5 Kim, S.-T. and O'Neil, J. R.: Equilibrium and non-equilibrium oxygen isotope effects in synthetic carbonates, *Geochim. Cosmochim. Acta*, 61, 3461–3475, 1997.
- Kluge, T., Marx, T., Scholz, D., Niggemann, S., Mangini, A., and Aeschbach-Hertig, W.: A new tool for palaeoclimate reconstruction: Noble gas temperatures from fluid inclusions in speleothems, *Earth Planet. Sc. Lett.*, 269, 408–415, doi:10.1016/j.epsl.2008.02.030, 2008.
- 10 Komadel, P. and Madejová, J.: Acid activation of clay minerals, in: *Handbook of Clay Science*, edited by: Bergaya, F., Theng, B. K. G., and Lagaly, G., *Developments in Clay Science*, Vol. 1, Elsevier Ltd., Amsterdam, 263–287, 2006.
- Kottek, M., Grieser, J., Beck, C., Rudolf, B., and Rubel, F.: World map of the Köppen-Geiger climate classification updated, *Meteorol. Z.*, 15, 259–263, doi:10.1127/0941-2948/2006/0130, 2006.
- 15 Krebs, W.: Massenkalk, in: *Geologische Karte von Nordrhein-Westfalen 1:25.000, Erläuterungen zu Blatt 4813 Attendorn, 2. Edn.*, edited by: Ziegler, W., Geologisches Landesamt Nordrhein-Westfalen, Krefeld, Germany, 78–94, 1978.
- Lachniet, M. S., Asmerom, Y., Burns, S. J., Patterson, W. P., Polyak, V. J., and Seltzer, G. O.: Tropical response to the 8200 yr B.P. cold event? Speleothem isotopes indicate a weakened early Holocene monsoon in Costa Rica, *Geology*, 32, 957–960, doi:10.1130/G20797.1, 2004.
- 20 Larrasoaña, J. C., Roberts, A. P., Rohling, E. J., Winkelhofer, M., and Wehausen, R.: Three million years of monsoon variability over the Northern Sahara, *Clim. Dynam.*, 21, 689–698, doi:10.1007/s00382-003-0355-z, 2003.
- Li, S.-L., Liu, C.-Q., Li, J., Lang, Y.-C., Ding, H., and Li, L.: Geochemistry of dissolved inorganic carbon and carbonate weathering in a small typical karstic catchment of Southwest China: Isotopic and chemical constraints, *Chem. Geol.*, 277, 301–309, doi:10.1016/j.chemgeo.2010.08.013, 2010.
- 30 Li, W., Chakraborty, S., Beard, B. L., Romanek, C. S., and Johnson, C. M.: Magnesium isotope fractionation during precipitation of inorganic calcite under laboratory conditions, *Earth Planet. Sc. Lett.*, doi:10.1016/j.epsl.2012.04.010, accepted, 2012.

The magnesium isotope record of cave carbonate archives

S. Riechelmann et al.

[Title Page](#)[Abstract](#)[Introduction](#)[Conclusions](#)[References](#)[Tables](#)[Figures](#)[⏪](#)[⏩](#)[◀](#)[▶](#)[Back](#)[Close](#)[Full Screen / Esc](#)[Printer-friendly Version](#)[Interactive Discussion](#)

Madejová, J., Bujdák, J., Janek, M., and Komadel, P.: Comparative FT-IR study of structural modifications during acid treatment of dioctahedral smectites and hectorite, *Spectrochim. Acta A*, 54, 1397–1406, 1998.

Mangini, A., Spötl, C., and Verdes, P.: Reconstruction of temperature in the Central Alps during the past 2000 yr from a $\delta^{18}\text{O}$ stalagmite record, *Earth Planet. Sc. Lett.*, 235, 741–751, doi:10.1016/j.epsl.2005.05.010, 2005.

Mangini, A., Verdes, P., Spötl, C., Scholz, D., Vollweiler, N., and Kromer, B.: Persistent influence of the North Atlantic hydrography on Central European winter temperature during the last 9000 years, *Geophys. Res. Lett.*, 34, L02704, doi:10.1029/2006GL028600, 2007.

Mann, M. E., Zhang, Z., Rutherford, S., Bradley, R. S., Hughes, M. K., Shindell, D., Ammann, C., Faluvegi, G., and Ni, F.: Global signatures and dynamical origins of the Little Ice Age and Medieval Climate Anomaly, *Science*, 326, 1256–1260, doi:10.1126/science.1177303, 2009.

Miorandi, R., Borsato, A., Frisia, S., Fairchild, I. J., and Richter, D. K.: Epikarst hydrology and implications for stalagmite capture of climate changes at Grotta di Ernesto (NE Italy): results from long-term monitoring, *Hydrol. Process.*, 24, 3101–3114, doi:10.1002/hyp.7744, 2010.

Mühlinghaus, C., Scholz, D., and Mangini, A.: Modelling stalagmite growth and $\delta^{13}\text{C}$ as a function of drip interval and temperature, *Geochim. Cosmochim. Acta*, 71, 2780–2790, doi:10.1016/j.gca.2007.03.018, 2007.

Negendank, J. F. W.: The Holocene: considerations with regard to its climate and climate archives, in: *The Climate in Historical Times – Towards a Synthesis of Holocene Proxy Data and Climate Models*, edited by: Fischer, H., Kumke, T., Lohmann, G., Flöser, G., Miller, H., von Storch, H., and Negendank, J. F. W., Springer, Berlin, 1–12, 2004.

Niggemann, S.: Klimabezogene Untersuchungen an spät- bis postglazialen Stalagmiten aus Massenkalkhöhlen des Sauerlandes, in: *Beiträge zur Speläologie I.*, edited by: Richter, D. K., and Wurth, G., Bochumer geol. u. geotechn. Arb., Bochum, 5–129, 2000.

Niggemann, S., Mangini, A., Mudelsee, M., Richter, D. K., and Wurth, G.: Sub-Milankovitch climatic cycles in Holocene stalagmites from Sauerland, Germany, *Earth Planet. Sc. Lett.*, 216, 539–547, doi:10.1016/S0012-821X(03)00513-2, 2003.

Okrusch, M. and Matthes, S.: *Mineralogie – eine Einführung in die spezielle Mineralogie, Petrologie und Lagerstättenkunde*, 7. Edn., Springer, Berlin, Heidelberg, New York, 526 pp., 2005.

The magnesium isotope record of cave carbonate archives

S. Riechelmann et al.

[Title Page](#)[Abstract](#)[Introduction](#)[Conclusions](#)[References](#)[Tables](#)[Figures](#)[⏪](#)[⏩](#)[◀](#)[▶](#)[Back](#)[Close](#)[Full Screen / Esc](#)[Printer-friendly Version](#)[Interactive Discussion](#)

- Pokrovsky, B. G., Mavromatis, V., and Pokrovsky, O. S.: Co-variation of Mg and C isotopes in late Precambrian carbonates of the Siberian platform: a new tool for tracing the change in weathering regime?, *Chem. Geol.*, 290, 67–74, doi:10.1016/j.chemgeo.2011.08.015, 2011.
- Polag, D., Scholz, D., Mühlinghaus, C., Spötl, C., Schröder-Ritzrau, A., Segl, M., and Mangini, A.: Stable isotope fractionation in speleothems: laboratory experiments, *Chem. Geol.*, 279, 31–39, doi:10.1016/j.chemgeo.2010.09.016, 2010.
- Reynard, L. M., Day, C. C., and Henderson, G. M.: Large fractionation of calcium isotopes during cave-analogue calcium carbonate growth, *Geochim. Cosmochim. Acta*, 75, 3726–3740, doi:10.1016/j.gca.2011.04.010, 2011.
- Richter, D. K., Meissner, P., Immenhauser, A., Schulte, U., and Dorsten, I.: Cryogenic and non-cryogenic pool calcites indicating permafrost and non-permafrost periods: a case study from the Herbstlabyrinth-Advent Cave system (Germany), *The Cryosphere*, 4, 501–509, doi:10.5194/tc-4-501-2010, 2010.
- Riechelmann, D. F. C.: Aktuospeläologische Untersuchungen in der Bunkerhöhle des Iserlohner Massenkalks (NRW/Deutschland): Signifikanz für kontinentale Klimaarchive, Ph. D. thesis, Fakultät für Geowissenschaften, Ruhr-Universität Bochum, Bochum, Germany, 199 pp., 2010.
- Riechelmann, D. F. C., Schröder-Ritzrau, A., Scholz, D., Fohlmeister, J., Spötl, C., Richter, D. K., and Mangini, A.: Monitoring Bunker Cave (NW Germany): a prerequisite to interpret geochemical proxy data of speleothems from this site, *J. Hydrol.*, 409, 682–695, 2011.
- Riechelmann, D. F. C., Deininger, M., Scholz, D., Riechelmann, S., Schröder-Ritzrau, A., Spötl, C., Richter, D. K., Immenhauser, A., and Mangini, A.: Disequilibrium carbon and oxygen isotope fractionation in recent cave calcite: comparison of cave precipitate and numerical model $\delta^{13}\text{C}$ and $\delta^{18}\text{O}$ data, *Geochim. Cosmochim. Acta*, in revision, 2012a.
- Riechelmann, S., Buhl, D., Schröder-Ritzrau, A., Spötl, C., Riechelmann, D. F. C., Richter, D. K., Kluge, T., Marx, T., and Immenhauser, A.: Hydrogeochemistry and fractionation pathways of Mg isotopes in a continental weathering system: lessons from field experiments, *Chem. Geol.*, 300–301, 109–122, doi:10.1016/j.chemgeo.2012.01.025, 2012b.
- Romanek, C. S., Grossman, E. L., and Morse, J. W.: Carbon isotopic formation in synthetic aragonite and calcite: effects of temperature and precipitation rate, *Geochim. Cosmochim. Acta*, 56, 419–430, 1992.

The magnesium isotope record of cave carbonate archives

S. Riechelmann et al.

[Title Page](#)
[Abstract](#)
[Introduction](#)
[Conclusions](#)
[References](#)
[Tables](#)
[Figures](#)




[Back](#)
[Close](#)
[Full Screen / Esc](#)
[Printer-friendly Version](#)
[Interactive Discussion](#)


- Rudzka, D., McDermott, F., Baldini, L. M., Fleitmann, D., Moreno, A., and Stoll, H.: The coupled $\delta^{13}\text{C}$ -radiocarbon systematics of three late glacial/early Holocene speleothems; insights into soil and cave processes at climate transition, *Geochim. Cosmochim. Acta*, 75, 4321–4339, doi:10.1016/j.gca.2011.05.022, 2011.
- 5 Sanchez, P. A. and Buol, S. W.: Properties of some soils of the upper Amazon basin of Peru, *Soil Sci. Soc. Am. Proc.*, 38, 117–121, 1974.
- Scheidegger, Y., Kluge, T., Kipfer, R., Aeschbach-Hertig, W., and Wieler, R.: Paleotemperature reconstruction using noble gas concentrations in speleothem fluid inclusions, *PAGES News*, 16, 10–12, 2008.
- 10 Scholz, D. and Hoffmann, D. L.: StalAge – an algorithm designed for construction of speleothem age models, *Quat. Geochronol.*, 6, 369–382, doi:10.1016/j.quageo.2011.02.002, 2011.
- Scholz, D., Mühlinghaus, C., and Mangini, A.: Modelling $\delta^{13}\text{C}$ and $\delta^{18}\text{O}$ in the solution layer on stalagmite surfaces, *Geochim. Cosmochim. Acta*, 73, 2592–2602, doi:10.1016/j.gca.2009.02.015, 2009.
- 15 Sherwin, C. M. and Baldini, J. U. L.: Cave air and hydrological controls on prior calcite precipitation and stalagmite growth rates: implications for palaeoclimate reconstructions using speleothems, *Geochim. Cosmochim. Acta*, 75, 3915–3929, doi:10.1016/j.gca.2011.04.020, 2011.
- Soon, W., Baliunas, S., Idso, C., Idso, S., and Legates, D. R.: Reconstructing climatic and environmental changes of the past 1000 years: a reappraisal, *Energy Environ.*, 14, 233–296, 2003.
- 20 Spötl, C. and Mangini, A.: Speleothems and paleoglaciators, *Earth Planet. Sc. Lett.*, 254, 323–331, 2007.
- Spötl, C., Mangini, A., Frank, N., Eichstädter, R., and Burns, S. J.: Start of the last interglacial period at 135 ka: evidence from a high alpine speleothem, *Geology*, 30, 815–818, 2002.
- 25 Spötl, C., Fairchild, I. J., and Tooth, A. F.: Cave air control on dripwater geochemistry, Obir Caves (Austria): implications for speleothem deposition in dynamically ventilated caves, *Geochim. Cosmochim. Acta*, 69, 2451–2468, doi:10.1016/j.gca.2004.12.009, 2005.
- Spötl, C., Holzkämper, S., and Mangini, A.: The last and the penultimate interglacial as recorded by speleothems from a climatically sensitive high-elevation cave site in the Alps, in: *The Climate of Past Interglacials*, edited by: Sirocko, F., Claussen, M., Litt, T., and Sánchez-Goñi, M. F., *Developments in Quaternary Science Series*, Vol. 7, Elsevier, Amsterdam, 471–491, 2007.
- 30

The magnesium isotope record of cave carbonate archives

S. Riechelmann et al.

[Title Page](#)
[Abstract](#)
[Introduction](#)
[Conclusions](#)
[References](#)
[Tables](#)
[Figures](#)
[Back](#)
[Close](#)
[Full Screen / Esc](#)
[Printer-friendly Version](#)
[Interactive Discussion](#)


Sträßer, M.: Klimadiagramm-Atlas der Erde Teil 1: Europa und Nordamerika. Monats- und Jahresmittelwerte von Temperatur und Niederschlag für den Zeitraum 1961–1990, Duisburger geographische Arbeiten, 18, edited by: Blotvogel, H. H., Eckart, K., Flüchter, W., Habrich, W., Sträßer, M., and Wagner, E., Dortmunder Vertrieb für Bau- und Planungsliteratur, Dortmund, 222 pp., 1998.

Sträßer, M.: Klimadiagramm-Atlas der Erde Teil 2: Asien, Lateinamerika, Afrika, Australien und Ozeanien, Polarländer. Monats- und Jahresmittelwerte von Temperatur und Niederschlag für den Zeitraum 1961–1990, Duisburger Geographische Arbeiten, 20, edited by: Blotvogel, H. H., Eckart, K., Flüchter, W., Habrich, W., Sträßer, M., and Wagner, E., Dortmunder Vertrieb für Bau- und Planungsliteratur, Dortmund, 254 pp., 1999.

Tipper, E. T., Galy, A., Gaillardet, J., Bickle, M. J., Elderfield, H., and Carder, E. A.: The magnesium isotope budget of the modern ocean: constraints from riverine magnesium isotope ratios, *Earth Planet. Sc. Lett.*, 250, 241–253, doi:10.1016/j.epsl.2006.07.037, 2006a.

Tipper, E. T., Galy, A., Gaillardet, J., Bickle, M. J., Elderfield, H., and Carder, E. A.: The magnesium isotope budget of the modern ocean: constraints from riverine magnesium isotope ratios, *Earth Planet. Sc. Lett.*, 250, 241–253, doi:10.1016/j.epsl.2006.07.037, 2006b.

Tipper, E. T., Galy, A., and Bickle, M. J.: Calcium and magnesium isotope systematics in rivers draining the Himalaya-Tibetan-plateau region: Lithological or fractionation control?, *Geochim. Cosmochim. Acta*, 72, 1057–1075, doi:10.1016/j.gca.2007.11.029, 2008.

Tipper, E. T., Gaillardet, J., Louvat, P., Campas, F., and White, A. F.: Mg isotope constraints on soil pore-fluid chemistry: evidence from Santa Cruz, California, *Geochim. Cosmochim. Acta*, 74, 3883–3896, doi:10.1016/j.gca.2010.04.021, 2010.

Tooth, A. F. and Fairchild, I. J.: Soil and karst aquifer hydrological controls on the geochemical evolution of speleothem-forming drip waters, Crag cave, Southwest Ireland, *J. Hydrol.*, 273, 51–68, 2003.

Tremaine, D. M., Froelich, P. N., and Wang, Y.: Speleothem calcite formed *in situ*: modern calibration of $\delta^{18}\text{O}$ and $\delta^{13}\text{C}$ paleoclimate proxies in a continuously-monitored natural cave system, *Geochim. Cosmochim. Acta*, 75, 4929–4950, doi:10.1016/j.gca.2011.06.005, 2011.

van Breukelen, M. R.: Peruvian stalagmites as archives of Holocene temperature and rainfall variability, Ph. D. thesis, Vrije Universiteit Amsterdam, Amsterdam, The Netherlands, 208 pp., 2009.

The magnesium isotope record of cave carbonate archives

S. Riechelmann et al.

Title Page

Abstract

Introduction

Conclusions

References

Tables

Figures

⏪

⏩

◀

▶

Back

Close

Full Screen / Esc

Printer-friendly Version

Interactive Discussion



- van Breukelen, M. R., Vonhof, H. B., Hellstrom, J. C., Wester, W. C. G., and Kroon, D.: Fossil dripwater in stalagmites reveals Holocene temperature and rainfall variation in Amazonia, *Earth Planet. Sc. Lett.*, 275, 54–60, doi:10.1016/j.epsl.2008.07.060, 2008.
- 5 Verheyden, S., Genty, D., Deflandre, G., Quinif, Y., and Keppens, E.: Monitoring climatological, hydrological and geochemical parameters in the Pèrè Noël cave (Belgium): implication for the interpretation of speleothem isotopic and geochemical time-series, *Int. J. Speleol.*, 37, 221–234, 2008.
- 10 Vollweiler, N., Scholz, D., Mühlinghaus, C., Mangini, A., and Spötl, C.: A precisely dated climate record for the last 9 kyr from three high alpine stalagmites, Spannagel cave, Austria, *Geophys. Res. Lett.*, 33, L20703, doi:10.1029/2006GL027662, 2006.
- Wassenburg, J. A., Immenhauser, A., Richter, D. K., Jochum, K. P., Fietzke, J., Goos, M., Scholz, D., and Sabaoui, A.: Climate and cave control on Pleistocene/Holocene calcite-to-aragonite transitions in speleothems from Morocco: elemental and isotopic evidence, *Geochim. Cosmochim. Acta*, in revision, 2012.
- 15 White, W. B.: Paleoclimate records from speleothems in limestone caves, in: *Studies of cave sediments*, edited by: Sasowsky, I. D. and Mylroie, J., Kluwer, New York, 135–176, 2004.
- Williams, P. W., King, D. N. T., Zhao, J. X., and Collerson, K. D.: Speleothem master chronologies: combined Holocene ^{18}O and ^{13}C records from the North Island of New Zealand and their palaeoenvironmental interpretation, *Holocene*, 14, 194–208, 2004.
- 20 Young, E. D. and Galy, A.: The isotope geochemistry and cosmochemistry of magnesium, *Rev. Mineral. Geochem.*, 55, 197–230, 2004.

The magnesium isotope record of cave carbonate archives

S. Riechelmann et al.

Table 1. Locality, hostrock composition, climate setting, weather stations and speleothems used in this paper. Asterisk (*) indicates data by Niggemann et al. (2003) and circle (°) indicates data by Spötl et al. (2002). Monitoring data for Bunker Cave represent the period 2006 to 2010 and monitoring data for Grotte Prison de Chien represent the period 2009 to 2011.

	Atta Cave, Rhenish Slate Mountains, Germany	Bunker Cave, Rhenish Slate Mountains, Germany	Cueva del Tigre Perdidó, Foothills of the Andes, Peru	Grotte d'Aoufous, Anti-Atlas, Morocco	Grotte Prison de Chien, Middle Atlas, Morocco	Spannagel Cave, Alps, Austria
Coordinates	51°7' N/7°55' E	51°22' N/7°40' E	6°54' S/78°18' W	–	–	47°5' N/11°40' E
Altitude of cave entrance (m a.s.l.)	265	184	1000	1000	360	2531
Hostrock	Massive, Middle Devonian limestone	Massive, Middle Devonian limestone	Massive, Triassic limestone	Massive, Upper Cretaceous limestone	Brecciated, Upper Jurassic limestone with subordinate dolomite	Calclitic, Jurassic marble
Climate after Kottek et al. (2006)	Warm temperate. Fully humid with warm summers	Warm temperate. Fully humid with warm summers	Equatorial. Fully humid with constantly warm temperatures	Arid. Desert, hot arid	Warm temperate. Dry and hot summers	Snow. Fully humid with cool summers
Cave air temperature (°C)	9.4*	10.8 (monitoring data)	–	–	13.9 (monitoring data)	1.2 to 2.2°
Mean annual temperature (°C)	9.1	9.9	22.6	20.9	17.6	–4.8
Annual precipitation (mm)	1172	971 (monitoring data)	1344	82	801	2004
Weatherstation	Olpe, Germany	Hagen-Fley/Hemer, Germany	Moyobamba, Peru	Bechar, Algeria	Taza, Morocco	Zugspitze, Germany
Coordinates of weatherstation	51°2' N/7°50' E	51°25' N/7°29' E/ 51°23' N/7°45' E	6°02' S/76°58' W	31°37' N/2°14' W	34°13' N/4°00' W	47°25' N/10°59' E
Altitude of weatherstation (m a.s.l.)	309	100/200	833	773	519	2962
Time period used	2003–2010	2006–2007/2008–2010	1961–1990	1961–1990	1961–1990	1961–1990
Data from	www.meteoedia.de	www.dwd.de/www.meteoedia.de	Sträßer (1999)	Sträßer (1999)	Sträßer (1999)	Sträßer (1998)
Speleothem, label	AH-1	BU 4	NC-A/NC-B	GDA	HK3	SPA 52/SPA 59
Speleothem, year of sampling	1997	2007	2003	2005	2009	2000
Speleothem, age (ka)	0.015–9	0.005–8.6	~ 0.009–4.3/3.2–14	2134 ± 115	4.24–27.48	92–212/54–247

Title Page

Abstract

Introduction

Conclusions

References

Tables

Figures



Back

Close

Full Screen / Esc

Printer-friendly Version

Interactive Discussion



The magnesium isotope record of cave carbonate archives

S. Riechelmann et al.

Title Page

Abstract

Introduction

Conclusions

References

Tables

Figures

⏪

⏩

◀

▶

Back

Close

Full Screen / Esc

Printer-friendly Version

Interactive Discussion



Table 2. Magnesium-isotope values of all speleothem samples. Repeated analyses are marked “wh” and mean values are indicated “mean”. $\Delta^{25}\text{Mg}$ data were calculated using the equations of Young and Galy (2004) in order to document the accuracy of analytical results. AH-1: 36 samples (July to August 2007), BU 4: 23 samples (February to March 2011), NC-A/NC-B: 3/6 samples (January to February 2008), GDA: 18 samples, June 2006), HK3: 6 samples (June 2011) and SPA 52/SPA 59: 8/12 samples, October 2009 to January 2010).

Speleothem	Sample	$\delta^{25}\text{Mg}$ (‰ DSM3)	$\pm 2\sigma$ (‰ DSM3)	$\delta^{26}\text{Mg}$	$\pm 2\sigma$	$\Delta^{25}\text{Mg}$
AH-1	09	-2.17	0.02	-4.18	0.05	0.01
AH-1	08	-2.13	0.01	-4.07	0.05	-0.01
AH-1	07	-2.14	0.02	-4.13	0.07	0.02
AH-1	06	-2.09	0.01	-4.02	0.04	0.00
AH-1	05	-2.11	0.02	-4.08	0.06	0.01
AH-1	04	-2.12	0.02	-4.14	0.04	0.04
AH-1	03	-2.14	0.02	-4.11	0.04	0.01
AH-1	02	-2.12	0.01	-4.11	0.07	0.02
AH-1	01	-2.10	0.01	-4.06	0.05	0.02
AH-1	1	-2.11	0.02	-4.06	0.05	0.01
AH-1	2	-2.05	0.02	-3.95	0.03	0.01
AH-1	3	-2.08	0.02	-4.00	0.03	0.01
AH-1	4	-2.07	0.03	-3.99	0.05	0.01
AH-1	5	-2.07	0.01	-4.01	0.02	0.02
AH-1	6	-2.07	0.02	-3.97	0.04	0.01
AH-1	7	-2.08	0.02	-4.00	0.02	0.01
AH-1	8	-2.07	0.02	-3.99	0.05	0.01
AH-1	9	-2.08	0.03	-4.03	0.03	0.02
AH-1	10	-2.08	0.03	-4.04	0.06	0.02
AH-1	11	-2.09	0.03	-4.02	0.04	0.00
AH-1	12	-2.08	0.02	-4.02	0.03	0.02
AH-1	13	-2.10	0.02	-4.04	0.02	0.01
AH-1	14	-2.10	0.04	-4.07	0.09	0.02
AH-1	14wh	-2.09	0.02	-4.02	0.03	0.01
AH-1	14 mean	-2.10	0.04	-4.05	0.09	0.01
AH-1	15	-2.07	0.03	-3.98	0.05	0.01
AH-1	16	-2.07	0.02	-3.95	0.02	-0.01
AH-1	17	-2.04	0.02	-3.93	0.03	0.01
AH-1	18	-2.10	0.01	-4.02	0.04	-0.01
AH-1	18wh	-2.05	0.02	-3.96	0.05	0.02
AH-1	18 mean	-2.08	0.04	-3.99	0.05	0.00
AH-1	19	-2.02	0.03	-3.89	0.08	0.00
AH-1	19wh	-2.04	0.03	-3.93	0.03	0.01
AH-1	19 mean	-2.03	0.03	-3.91	0.08	0.01
AH-1	20	-2.04	0.03	-3.93	0.04	0.01
AH-1	21	-2.06	0.02	-3.97	0.06	0.01
AH-1	22	-2.06	0.02	-3.98	0.03	0.01
AH-1	23	-2.06	0.02	-3.98	0.05	0.02
AH-1	24	-2.08	0.03	-3.97	0.05	-0.01
AH-1	25	-2.00	0.02	-3.87	0.05	0.02
AH-1	25wh	-1.99	0.02	-3.86	0.03	0.02
AH-1	25 mean	-1.99	0.02	-3.87	0.05	0.03
AH-1	26	-2.06	0.02	-3.98	0.05	0.02
AH-1	27	-2.05	0.04	-3.94	0.07	0.01

Table 2. Continued.

Speleothem	Sample	$\delta^{26}\text{Mg}$ (‰ DSM3)	$\pm 2\sigma$ (‰ DSM3)	$\delta^{26}\text{Mg}$	$\pm 2\sigma$	$\Delta^{26}\text{Mg}^1$
BU 4	0	-2.09	0.02	-4.02	0.02	0.01
BU 4	1	-2.14	0.02	-4.12	0.03	0.01
BU 4	2	-2.23	0.02	-4.29	0.06	0.00
BU 4	3	-2.14	0.02	-4.13	0.02	0.01
BU 4	4	-2.24	0.03	-4.29	0.04	0.00
BU 4	5	-2.18	0.02	-4.21	0.03	0.01
BU 4	6	-2.01	0.02	-3.91	0.05	0.03
BU 4	7	-2.13	0.02	-4.12	0.03	0.02
BU 4	8	-2.17	0.02	-4.18	0.03	0.01
BU 4	9	-2.19	0.03	-4.22	0.06	0.01
BU 4	10	-2.24	0.02	-4.32	0.02	0.01
BU 4	11	-2.19	0.02	-4.21	0.02	0.01
BU 4	12	-2.22	0.01	-4.26	0.03	0.00
BU 4	13	-2.19	0.02	-4.21	0.06	0.01
BU 4	13A	-2.16	0.01	-4.18	0.02	0.02
BU 4	14	-2.20	0.01	-4.24	0.02	0.01
BU 4	14A	-2.17	0.02	-4.17	0.05	0.01
BU 4	15	-2.24	0.01	-4.31	0.01	0.00
BU 4	15A	-2.12	0.02	-4.08	0.02	0.00
BU 4	16	-2.19	0.02	-4.22	0.02	0.01
BU 4	16A	-2.26	0.06	-4.34	0.07	0.00
BU 4	17	-2.21	0.02	-4.26	0.01	0.01
BU 4	17A	-2.21	0.01	-4.27	0.01	0.02
NC-A	0-0.5 cm	-2.00	0.03	-3.88	0.03	0.02
NC-A	10-10.5 cm	-2.08	0.02	-4.03	0.04	0.02
NC-A	20-20.5 cm	-2.03	0.01	-3.92	0.01	0.02
NC-B	0.5-01 cm	-2.05	0.02	-3.96	0.05	0.01
NC-B	5-5.5 cm	-2.05	0.02	-3.97	0.03	0.02
NC-B	11.5-12 cm	-2.08	0.02	-3.99	0.01	0.00
NC-B	18.5-19 cm	-2.03	0.03	-3.96	0.06	0.03
NC-B	18.5-19 cm wh	-2.04	0.02	-3.94	0.03	0.01
NC-B	18.5-19 cm mean	-2.04	0.03	-3.95	0.06	0.02
NC-B	25.5-26 cm	-2.07	0.02	-4.00	0.04	0.01
NC-B	28.5-29 cm	-2.05	0.02	-3.96	0.03	0.02
GDA	pos 3/4	-2.22	0.03	-4.28	0.04	0.02
GDA	pos 5	-2.24	0.02	-4.33	0.04	0.01
GDA	pos 10	-2.28	0.02	-4.38	0.05	0.01
GDA	pos 17	-2.27	0.02	-4.39	0.02	0.01
GDA	pos 22a	-2.19	0.02	-4.23	0.03	0.01
GDA	pos 25	-2.21	0.02	-4.26	0.04	0.01
GDA	pos 30	-2.17	0.01	-4.17	0.05	0.01
GDA	pos 37	-2.20	0.02	-4.23	0.06	0.01
GDA	pos 45	-2.25	0.02	-4.31	0.08	0.00
GDA	pos 14/15	-2.26	0.02	-4.35	0.05	0.01
GDA	pos 20	-2.23	0.03	-4.26	0.04	-0.01
GDA	pos 40	-2.16	0.02	-4.18	0.03	0.02
GDA	pos 33a	-2.19	0.01	-4.22	0.01	0.02
GDA	pos 33b	-2.18	0.01	-4.20	0.03	0.01
GDA	pos 33e	-2.17	0.02	-4.19	0.03	0.01
GDA	pos 33d	-2.18	0.03	-4.21	0.03	0.01
GDA	pos 33f	-2.19	0.01	-4.22	0.02	0.01
GDA	pos 33c	-2.18	0.02	-4.19	0.04	0.01

The magnesium isotope record of cave carbonate archives

S. Riechelmann et al.

Title Page

Abstract

Introduction

Conclusions

References

Tables

Figures

⏪

⏩

◀

▶

Back

Close

Full Screen / Esc

Printer-friendly Version

Interactive Discussion



Table 2. Continued.

Speleothem	Sample	$\delta^{26}\text{Mg}$ (‰ DSM3)	$\pm 2\sigma$ (‰ DSM3)	$\delta^{26}\text{Mg}$	$\pm 2\sigma$	$\Delta^{26}\text{Mg}^1$
HK3	CA24	-2.02	0.03	-3.89	0.06	0.01
HK3	CA37	-2.20	0.03	-4.21	0.07	-0.01
HK3	CA41	-2.23	0.01	-4.29	0.02	0.00
HK3	CA45	-2.22	0.04	-4.27	0.09	0.00
HK3	CA63	-2.23	0.02	-4.26	0.04	0.00
HK3	CA74	-2.16	0.02	-4.13	0.03	-0.01
SPA 52	a	-1.48	0.02	-2.84	0.06	0.00
SPA 52	b	-1.35	0.03	-2.62	0.06	0.02
SPA 52	c	-1.61	0.02	-3.11	0.02	0.01
SPA 52	g	-1.8	0.02	-3.47	0.04	0.01
SPA 52	d	-1.72	0.03	-3.33	0.02	0.02
SPA 52	h	-1.86	0.09	-3.58	0.14	0.01
SPA 52	e	-1.89	0.05	-3.63	0.05	0.00
SPA 52	f	-0.73	0.02	-1.42	0.04	0.01
SPA 59	a	-2.10	0.02	-4.06	0.04	0.02
SPA 59	aa	-1.96	0.04	-3.80	0.07	0.02
SPA 59	ab	-2.05	0.03	-3.97	0.02	0.02
SPA 59	ac	-2.07	0.05	-3.99	0.09	0.01
SPA 59	ad	-1.96	0.03	-3.80	0.04	0.02
SPA 59	ae	-1.93	0.05	-3.70	0.07	0.00
SPA 59	b	-1.29	0.03	-2.47	0.05	0.00
SPA 59	c	-2.06	0.02	-3.97	0.07	0.01
SPA 59	d	-1.86	0.03	-3.59	0.06	0.01
SPA 59	da	-1.79	0.02	-3.43	0.03	0.00
SPA 59	e	-1.99	0.01	-3.83	0.03	0.01
SPA 59	f	-1.96	0.04	-3.78	0.06	0.01

The magnesium isotope record of cave carbonate archives

S. Riechelmann et al.

Title Page

Abstract

Introduction

Conclusions

References

Tables

Figures

⏪

⏩

◀

▶

Back

Close

Full Screen / Esc

Printer-friendly Version

Interactive Discussion



The magnesium isotope record of cave carbonate archives

S. Riechelmann et al.

Table 3. Mean Mg-isotope ratios, minimum and maximum values and $\Delta^{26}\text{Mg}$ (difference between maximum and minimum value) of speleothems discussed here. Number of samples used for statistics varies between 6 and 36.

$\delta^{26}\text{Mg}$ (‰ DSM3)	AH-1	BU 4	NC-A/NC-B	GDA	HK3	SPA 52	SPA 59
Mean	-4.01 ± 0.07	-4.20 ± 0.10	-3.96 ± 0.04	-4.26 ± 0.07	-4.17 ± 0.15	-3.00 ± 0.73	-3.70 ± 0.43
min	-4.18 ± 0.05	-4.34 ± 0.07	-4.03 ± 0.04	-4.39 ± 0.02	-4.29 ± 0.02	-3.63 ± 0.05	-4.06 ± 0.04
max	-3.86 ± 0.03	-3.91 ± 0.05	-3.88 ± 0.03	-4.17 ± 0.05	-3.89 ± 0.06	-1.42 ± 0.04	-2.47 ± 0.05
$\Delta^{26}\text{Mg}$	0.32	0.44	0.14	0.22	0.40	2.21	1.59

Title Page

Abstract

Introduction

Conclusions

References

Tables

Figures

◀

▶

◀

▶

Back

Close

Full Screen / Esc

Printer-friendly Version

Interactive Discussion

The magnesium isotope record of cave carbonate archives

S. Riechelmann et al.

Table 4. Magnesium isotope composition of several samples of the stalagmite AH-1 measured with and without fluid inclusions and the calculated $\Delta^{26}\text{Mg}$ between these samples.

Speleothem	Sample	$\delta^{26}\text{Mg}$ (‰ DSM3) total sample	$\pm 2\sigma$	$\delta^{26}\text{Mg}$ (‰ DSM3) without fluids	$\pm 2\sigma$	$\Delta^{26}\text{Mg}$
AH-1	05	−4.08	0.06	−4.10	0.02	0.03
AH-1	2	−3.95	0.03	−3.97	0.05	0.02
AH-1	4	−3.99	0.05	−4.00	0.05	0.01
AH-1	6	−3.97	0.04	−4.03	0.01	0.06
AH-1	17	−3.93	0.03	−4.00	0.06	0.08
AH-1	23	−3.98	0.05	−4.03	0.02	0.05
AH-1	24	−3.97	0.05	−3.98	0.05	0.02
AH-1	26	−3.98	0.05	−4.01	0.04	0.03
AH-1	27	−3.94	0.07	−3.98	0.02	0.03

Title Page

Abstract

Introduction

Conclusions

References

Tables

Figures

⏪

⏩

◀

▶

Back

Close

Full Screen / Esc

Printer-friendly Version

Interactive Discussion



The magnesium isotope record of cave carbonate archives

S. Riechelmann et al.

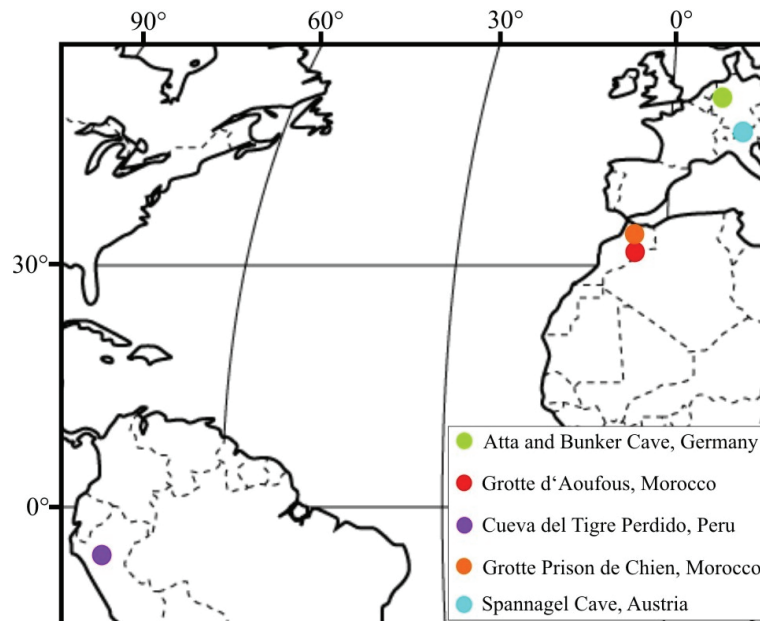


Fig. 1. Map with the locations of studied caves. Atta and Bunker Cave (Germany) are represented by a single green dot.

[Title Page](#)[Abstract](#)[Introduction](#)[Conclusions](#)[References](#)[Tables](#)[Figures](#)[⏪](#)[⏩](#)[⏴](#)[⏵](#)[Back](#)[Close](#)[Full Screen / Esc](#)[Printer-friendly Version](#)[Interactive Discussion](#)

The magnesium isotope record of cave carbonate archives

S. Riechelmann et al.

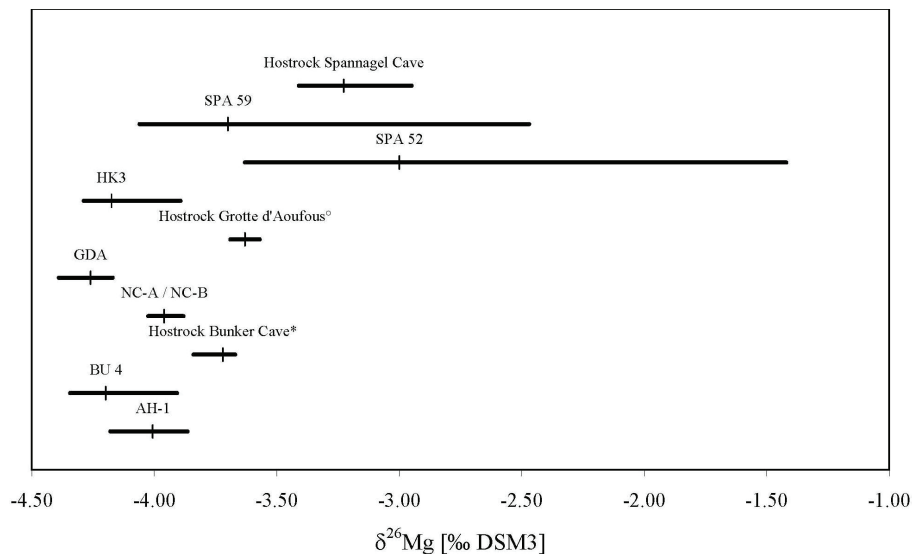


Fig. 2. Overview of Mg-isotope data of the studied speleothems and hostrock. Mean value is indicated by thin vertical line, width of horizontal bars indicate data range. Asterisk (*) indicates data from Immenhauser et al. (2010) and circle (°) indicates data from Buhl et al. (2007).

Title Page

Abstract

Introduction

Conclusions

References

Tables

Figures

◀

▶

◀

▶

Back

Close

Full Screen / Esc

Printer-friendly Version

Interactive Discussion



The magnesium isotope record of cave carbonate archives

S. Riechelmann et al.

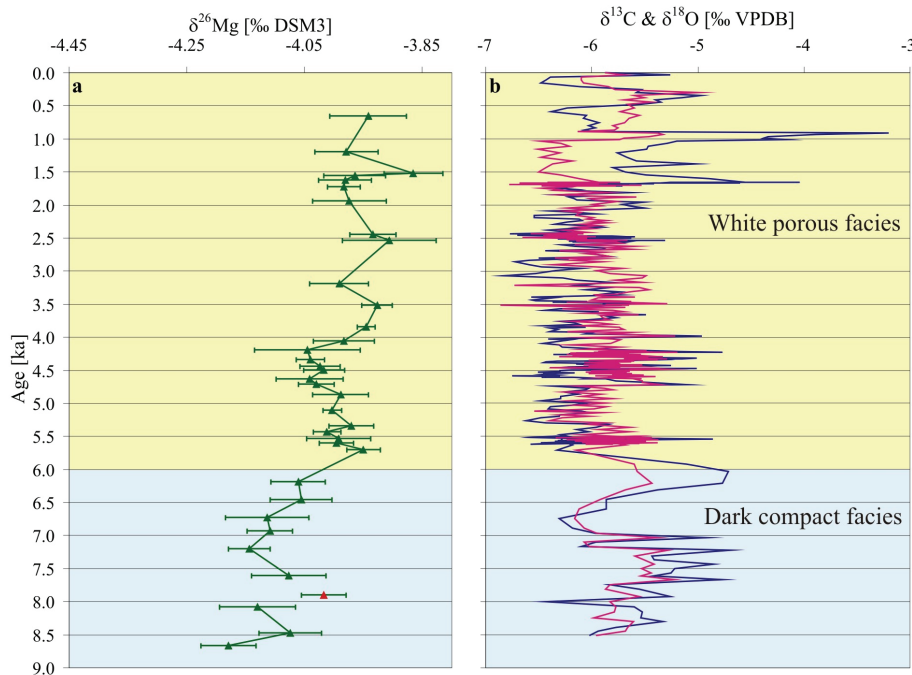


Fig. 3. Magnesium, carbon and oxygen isotope data of the stalagmite AH-1 from Atta Cave, Germany. **(a)** Mg-isotope data plotted against age in ka BP using the StalAge model of Scholz and Hoffmann (2011). Red triangle indicates sample taken in a detritus layer. **(b)** Carbon (dark blue) and oxygen (magenta) isotope data plotted against age in ka BP (data from Niggemann et al., 2003). Portions of the speleothem characterized by a dark compact facies are shown in blue, those characterized by a white porous facies are shown in yellow.

Title Page

Abstract

Introduction

Conclusions

References

Tables

Figures

◀

▶

◀

▶

Back

Close

Full Screen / Esc

Printer-friendly Version

Interactive Discussion

The magnesium isotope record of cave carbonate archives

S. Riechelmann et al.

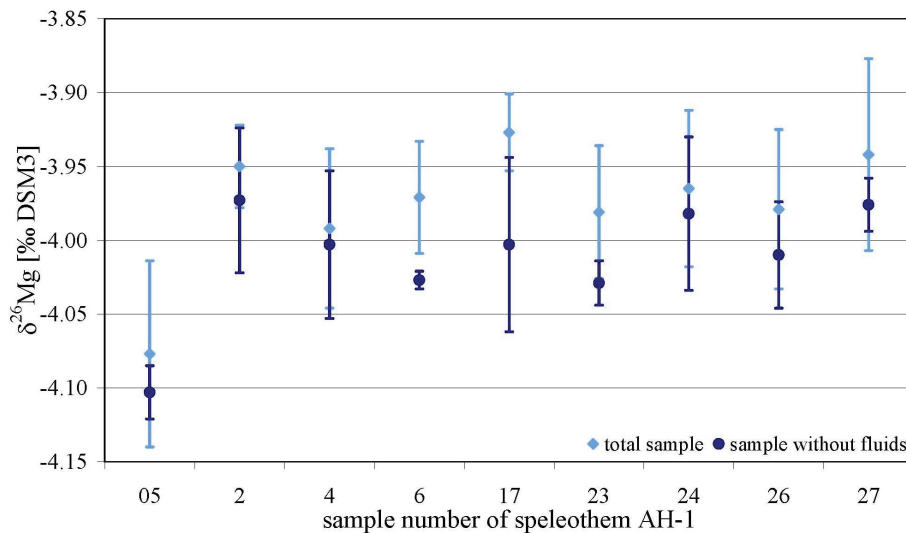


Fig. 4. Magnesium isotope composition of aliquots of samples from stalagmite AH-1. Dark blue indicates crushed samples in order to remove fluid inclusions whilst light blue indicates bulk samples. Note systematic offset.

[Title Page](#)[Abstract](#)[Introduction](#)[Conclusions](#)[References](#)[Tables](#)[Figures](#)[◀](#)[▶](#)[◀](#)[▶](#)[Back](#)[Close](#)[Full Screen / Esc](#)[Printer-friendly Version](#)[Interactive Discussion](#)

The magnesium isotope record of cave carbonate archives

S. Riechelmann et al.

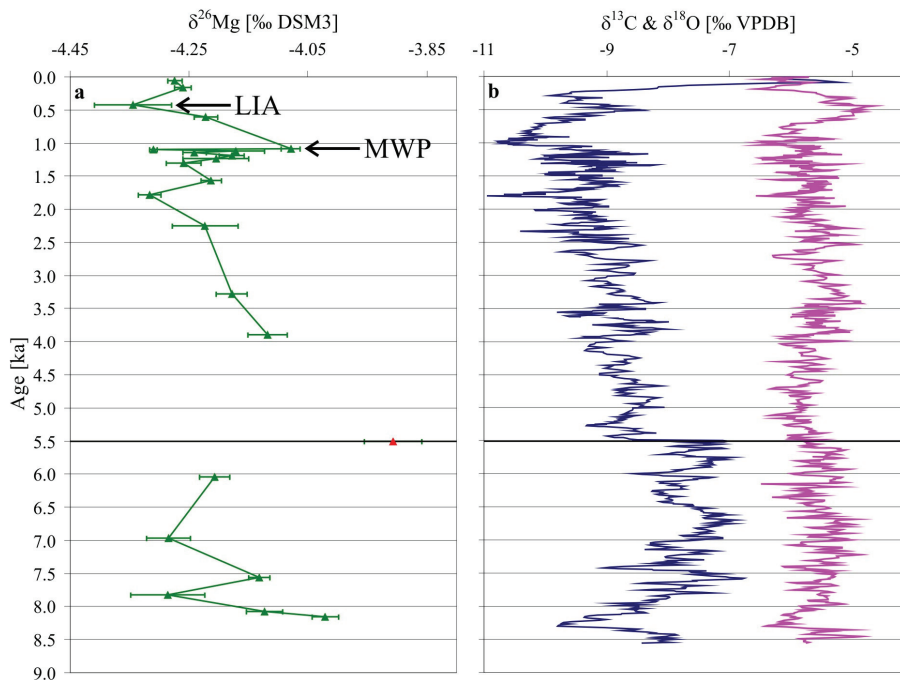


Fig. 5. Magnesium, carbon and oxygen isotope data of the stalagmite BU 4 from Bunker Cave, Germany. Black line marks hiatus characterized by a coralloid layer and detrital material. **(a)** Mg-isotope data plotted against age in ka BP. Red triangle indicates sample taken in a detritus layer. **(b)** Carbon (dark blue) and oxygen (magenta) isotope data plotted against age in ka BP (data from Fohlmeister et al., 2012). Samples taken at the time of the Medieval Warm Period (MWP) and of the Little Ice Age (LIA) are indicated with black arrows.

Title Page

Abstract

Introduction

Conclusions

References

Tables

Figures

◀

▶

◀

▶

Back

Close

Full Screen / Esc

Printer-friendly Version

Interactive Discussion

The magnesium isotope record of cave carbonate archives

S. Riechelmann et al.

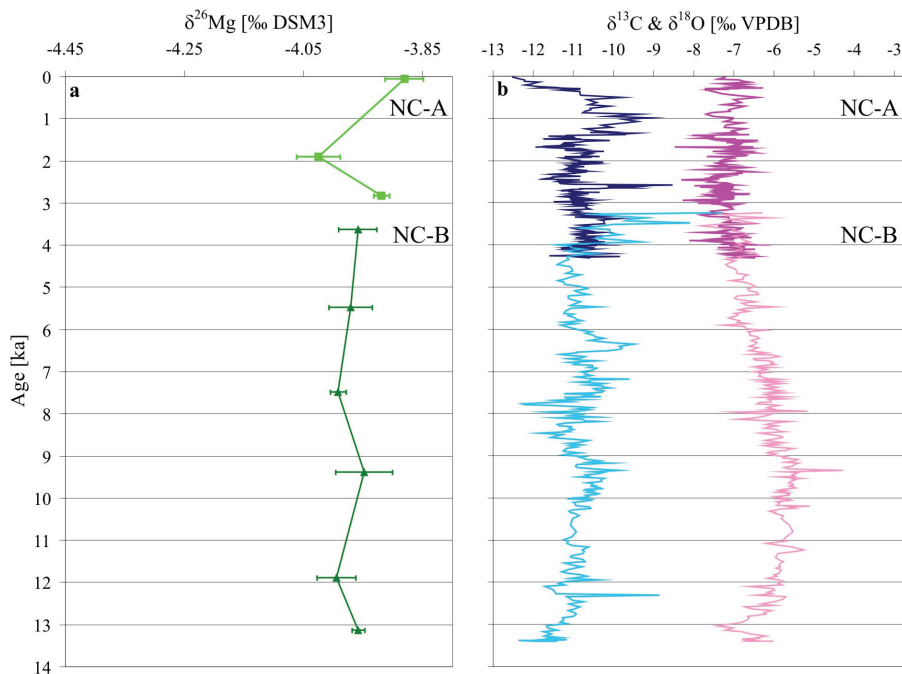


Fig. 6. Magnesium, carbon and oxygen isotope data of stalagmites NC-A and NC-B from Cueva del Tigre Perdido, Peru. **(a)** Mg-isotope data (NC-A: light green squares; NC-B: green triangles) plotted against age in ka BP using the StalAge model of Scholz and Hoffmann (2011). **(b)** Carbon (NC-A: dark blue; NC-B: light blue) and oxygen (NC-A: magenta; NC-B: light magenta) isotope data plotted against age in ka BP (data from van Breukelen et al., 2008; van Breukelen, 2009).

Title Page

Abstract

Introduction

Conclusions

References

Tables

Figures

⏪

⏩

◀

▶

Back

Close

Full Screen / Esc

Printer-friendly Version

Interactive Discussion

The magnesium isotope record of cave carbonate archives

S. Riechelmann et al.

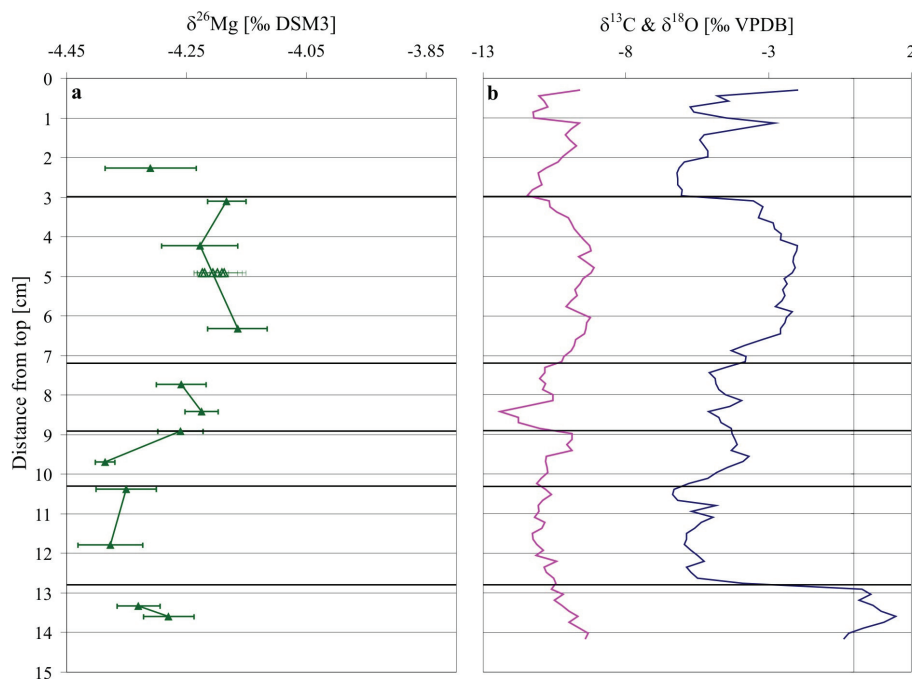


Fig. 7. Magnesium, carbon and oxygen isotope data of the stalagmite GDA from Grotte d'Aoufous, Morocco. Black lines mark hiatus. **(a)** Mg-isotope data are plotted against distance from top in cm. Open triangles indicate multiple samples along a single growth layer (Buhl et al., 2007). **(b)** Carbon (dark blue) and oxygen (magenta) isotope data plotted against distance from top in cm (data from Buhl et al., 2007).

[Title Page](#)[Abstract](#)[Introduction](#)[Conclusions](#)[References](#)[Tables](#)[Figures](#)[◀](#)[▶](#)[◀](#)[▶](#)[Back](#)[Close](#)[Full Screen / Esc](#)[Printer-friendly Version](#)[Interactive Discussion](#)

The magnesium isotope record of cave carbonate archives

S. Riechelmann et al.

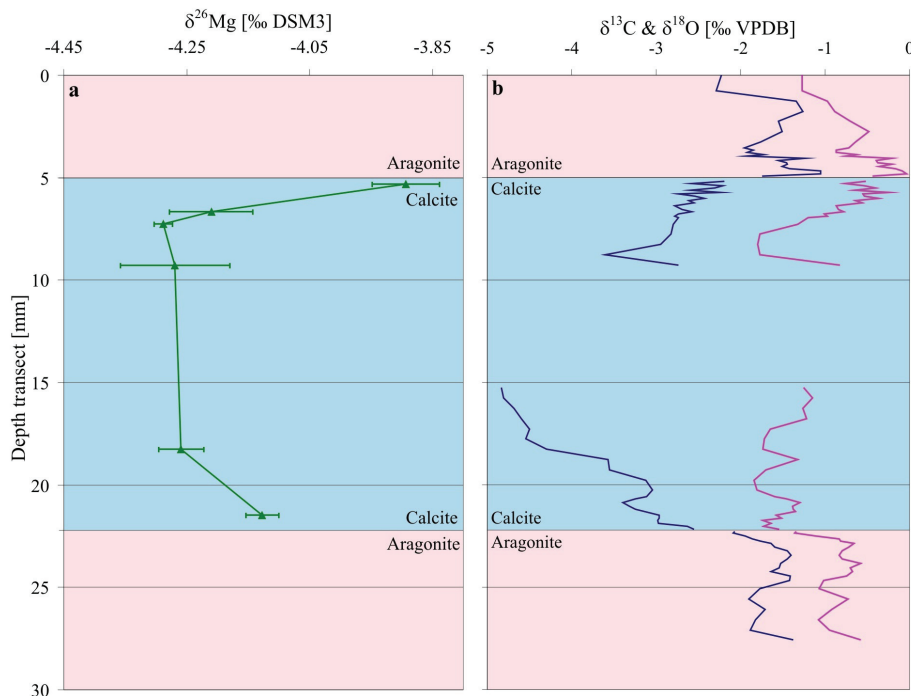


Fig. 8. Magnesium, carbon and oxygen data of the stalagmite HK3 from Grotte Prison de Chien, Morocco. **(a)** Mg-isotope data plotted against depth of the transect (top at 0 mm). **(b)** Carbon (dark blue) and oxygen (magenta) isotope data plotted against depth (data from Wassenburg et al., 2012). Colour code refers to aragonite or calcite intervals.

[Title Page](#)[Abstract](#)[Introduction](#)[Conclusions](#)[References](#)[Tables](#)[Figures](#)[◀](#)[▶](#)[◀](#)[▶](#)[Back](#)[Close](#)[Full Screen / Esc](#)[Printer-friendly Version](#)[Interactive Discussion](#)

The magnesium isotope record of cave carbonate archives

S. Riechelmann et al.

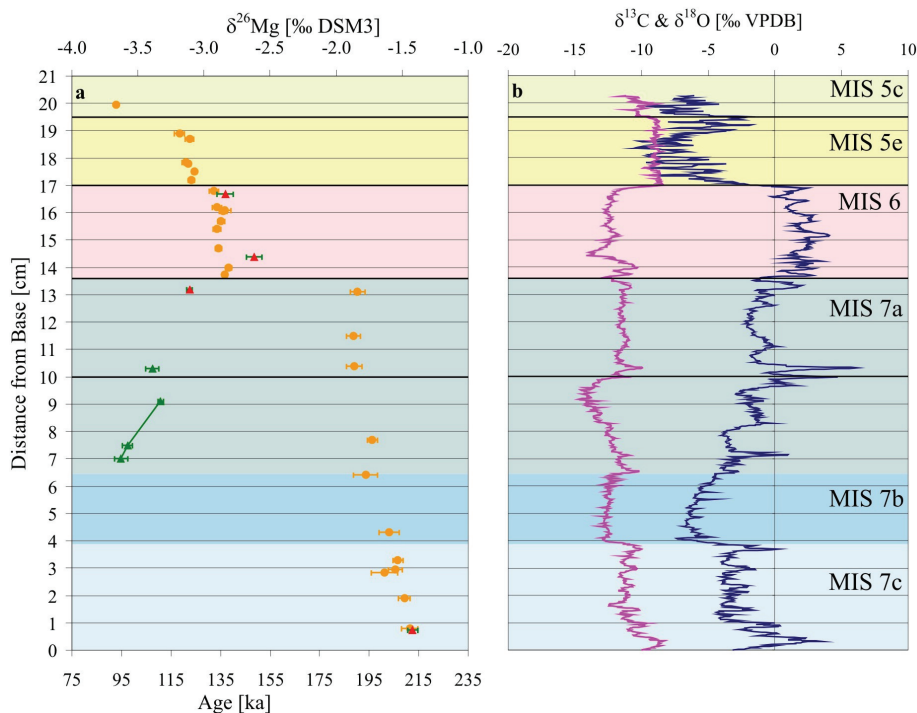


Fig. 9. Magnesium, age, carbon and oxygen isotope data of flowstone SPA 52 from Spannagel Cave, Austria. Thick black lines indicate hiatus. **(a)** Mg-isotope data (green) and age data (orange) plotted against distance from base in cm (age data from Spötl et al., 2007). Red triangles indicate samples taken in detritus layers. **(b)** Carbon (dark blue) and oxygen (magenta) isotope data plotted against distance from base in cm (data from Spötl et al., 2007). Marine isotope stages (MIS) after Spötl et al. (2007).

Title Page

Abstract

Introduction

Conclusions

References

Tables

Figures

◀

▶

◀

▶

Back

Close

Full Screen / Esc

Printer-friendly Version

Interactive Discussion

The magnesium isotope record of cave carbonate archives

S. Riechelmann et al.

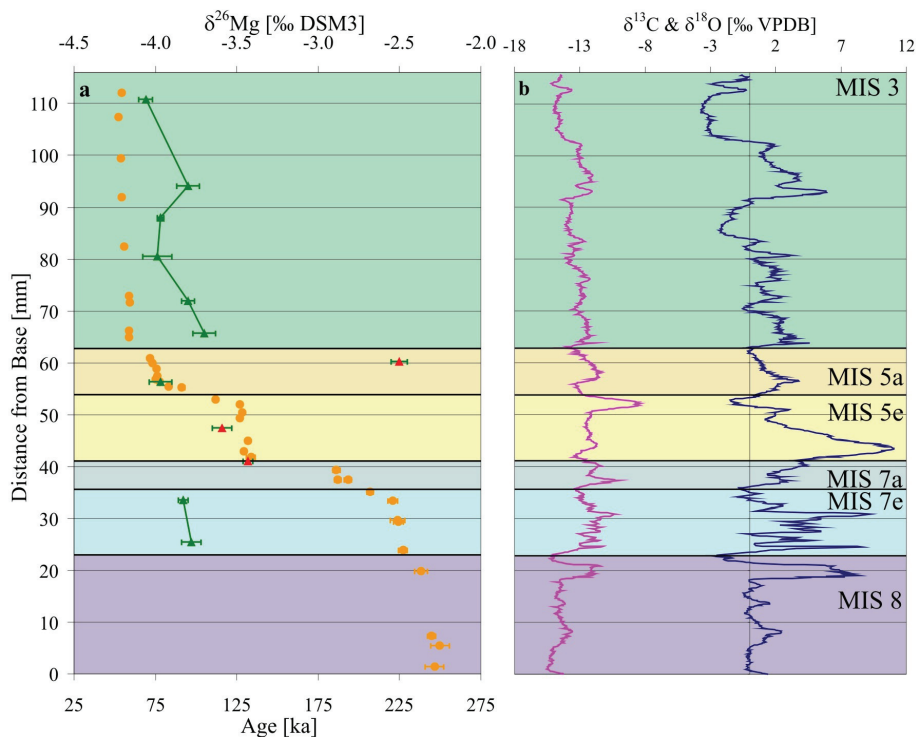


Fig. 10. Magnesium, age, carbon and oxygen isotope data of flowstone SPA 59 from Spannagel Cave, Austria. Thick black lines indicate hiatus. **(a)** Mg-isotope data (green) and age data (orange) plotted against distance from base in mm (age data from Holzschläger et al., 2005). Red triangles indicate samples taken in detritus layers. **(b)** Carbon (dark blue) and oxygen (magenta) isotope data plotted against distance from base in mm (data from Holzschläger et al., 2005). Marine isotope stages after Spötl et al. (2007).

Title Page

Abstract

Introduction

Conclusions

References

Tables

Figures

◀

▶

◀

▶

Back

Close

Full Screen / Esc

Printer-friendly Version

Interactive Discussion

